UNIVERSITY OF CALIFORNIA
SANTA CRUZ

MOLECULAR MECHANISMS FOR MEASURING AND LINKING CELL GROWTH TO MITOTIC PROGRESSION IN BUDDING YEAST

A dissertation submitted in partial
satisfaction of the requirements for the
degree of

DOCTOR OF PHILOSOPHY

in

MOLECULAR, CELL, AND DEVELOPMENTAL BIOLOGY

by

Francisco Javier Mendez Diaz

June 2023

The Dissertation of Francisco Mendez Diaz is approved:

_____
Professor Doug Kellogg, chair

_____
Professor Carrie Partch

_____
Professor Seth Rubin

_____
Peter Biehl
Vice Provost and Dean of Graduate Studies

Table of Contents

List of Figures/Tables…… v

Abstract…….. viii

Dedication…… x

Acknowledgements…….. xi

Chapter 1: Introduction……. 1

Regulation of cell size and growth…… 1

Growth-dependent signaling hypothesis……2

The Gin4 kinase as a growth sensor in mitosis…… 5

Importance of studying cell growth…… 8

Chapter 2: Mechanisms of growth-dependent activation of the Gin4 kinase……. 12

Introduction…… 9

Results…… 13

Materials and Methods…… 22

Figures…… 30

Chapter 3: Identification of Gin4-binding proteins via affinity mass spectrometry (unpublished data)…… 38

Introduction/Results…… 38

Materials and Methods…… 48

Figures…… 57

Tables…… 62

Table legends…… 65

Chapter 4: Effects of Gin4 C-terminal truncations on cell size and mitotic progression (unpublished data)…… 66

Introduction…… 66

Results…… 66

Materials and Methods…… 73

Figures…… 77

Chapter 5: Structural Model of a Gin4-Nap1 complex in the G1 phase of the cell cycle (unpublished data)……81

Introduction…… 81

Results…… 82

Materials and Methods…… 85

Figures…… 87

Bibliography……..…….91

List of Figures and Tables

Chapter 1

Figure A. Schematic of the budding yeast cell cycle …… 3

Figure B. Schematic of the growth-dependent signaling hypothesis…… 4

Chapter 2

Figure 1. Coomassie-stained gel image of purified Gin4-Nap1 complex…… 31

Figure 2. Phosphatidylserine binding to the KA1 domain is not sufficient to drive Gin4 hyperphosphorylation *in vitro*…… 32

Figure 3. Elm1 directly stimulates Gin4 autophosphorylation *in vitro*…… 33

Figure 4. Yck1/2 kinase activity is required for Gin4 hyperphosphorylation and normal mitotic progression *in vivo*…… 34

Figure 5. Yck1/2 localization to the plasma membrane is required for Gin4 hyperphosphorylation and normal mitotic progression *in vivo*…… 35

Figure 6. Yck1 stimulates Gin4 autophosphorylation in an Elm1-dependent manner *in vitro*…… 36

Figure 7. Yck1 promotes hyperphosphorylation and activation of Elm1 in *vivo and in vitro*…… 37

Figure 8. Model for growth-dependent phosphorylation and activation of Gin4 to promote mitotic progression…… 38

Chapter 3

Figure 1. Purification of recombinant wild type and kinase dead GST-tagged Gin4 kinases from *E. coli*…… 58

Figure 2. Purification of Gin4-binding proteins via sequential Gin4 affinity chromatography…… 59

Figure 3. Septin-Gin4 interactions are dependent on Gin4 kinase activity…… 60

Figure 4. Testing kinase candidates from the mass spectrometry analysis for the genetic requirement of Gin4 hyperphosphorylation *in vivo*…… 61

Figure 5. Testing phosphatase candidates from the mass spectrometry analysis for the genetic requirement of Gin4 hyperphosphorylation *in vivo*…… 62

Table 1. List of kinase candidates from Gin4 affinity mass spectrometry experiment…… 63

Table 2. List of phosphatase candidates from Gin4 affinity mass spectrometry experiment…… 64

Table 3. List of ribosome biogenesis candidates from Gin4 affinity mass spectrometry experiment…… 65

Chapter 4

Figure 1. Schematic of Gin4 C-terminal truncations…… 78

Figure 2. Effects on cell size in Gin4 C-terminal truncation yeast strains…… 79

Figure 3. Effects on mitotic progression in Gin4 C-terminal truncation yeast strains…… 80

Figure 4. Effects on growth rate in Gin4 C-terminal truncation yeast strains…… 81

Chapter 5

Figure 1. Coomassie-stained gel image of purified Gin4-Nap1 complex…… 88

Figure 2. Schematic of Cryo-EM workflow…… 89

Figure 3. 2D Classifications of Gin4-Nap1 particles…… 90

Figure 4. Model of Gin4-Nap1 structure in G1 phase of the cell cycle…… 91

Abstract

Molecular mechanisms for measuring and linking cell growth to mitotic progression in budding yeast

By Francisco Mendez Diaz

Cell cycle progression is dependent upon cell growth. Cells must, therefore, translate growth into a proportional signal that can be used to determine when sufficient growth has occurred for cell cycle progression. In budding yeast, a protein kinase called Gin4 is required for normal control of cell growth and undergoes gradual hyperphosphorylation that is dependent upon and proportional to added membrane growth in metaphase within the mitotic phase of the cell cycle. These observation suggest that growth-dependent phosphorylation of Gin4 could play a role in mechanisms that measure cell growth in mitosis. However, the molecular mechanisms that drive growth-dependent hyperphosphorylation of Gin4 are poorly understood. Here, we utilized a combination of biochemical reconstitution and genetic analysis to define the molecular mechanisms that drive growth dependent phosphorylation of Gin4. Our working model is that lipid vesicles that drive plasma membrane growth drive also deliver key signaling molecules that drive Gin4 hyperphosphorylation, which would suggest a simple mechanistic explanation for how growth-dependent Gin4 phosphorylation signals are generated. Gin4 has a KA1 domain that binds phosphatidylserine lipid and is required for growth-dependent phosphorylation of Gin4. Our work rules out a simple model in which phosphatidylserine delivered to sites of membrane growth binds and activates Gin4 to undergo autophosphorylation. Rather, the data suggest that phosphatidylserine

recruits Gin4 to sites of membrane growth, where it is phosphorylated and activated by Elm1 in a Yck1-dependent manner. In this manner, Gin4 phosphorylation signals are generated to drive inhibition of the mitotic inhibitor Swe1 to promote the metaphase to anaphase transition, allowing cells to complete division.

Dedication

Para mi abuelita Victoria. Te amo y te extraño muchísimo.

Acknowledgements

It has been a long journey! From being the first person in my family to pursue a Ph.D. to becoming a father. It has been a joyful, but stressful ride in graduate school. There have been many times during graduate school where I felt like I did not belong in academia, and I really considered dropping out. However, I have had and still have an amazing support system that kept me motivated every day to continue working hard towards earning my Ph.D. I would like to take this space to thank many people who supported me throughout my life. Without my support system, I would not be here earning a Ph.D. in science.

First, I would like to thank all the friends I have made throughout my grade school years and those I made in college for believing in me. Three people that made my life so much easier during high school are Miguel Hernandez, Monica Espinoza, and Kevin Guthrie. I thank them very much for looking out for me when my parents were deported to Mexico. Thank you for supporting and acknowledging my desire to pursue a career in science. I would also like to thank the brothers of Gamma Zeta Alpha Fraternity, a brotherhood I joined at UC San Diego during my undergraduate years, for making me the man I am today. From the fraternity, I learned how to be a professional, how to value diversity, and how to serve communities. I wouldn't be able to communicate my scientific research without the qualities I obtained as a member of Gamma Zeta Alpha Fraternity.

Second, I would like to thank all my mentors at UC San Diego. Especially, I would like to give a big thank you to Dr. Antonio DeMaio for introducing me to the research world during my undergraduate years and providing me with an opportunity to learn the basics of biomedical research in his laboratory. I would also like to thank Dr. DeMaio for offering an opportunity to join the IMSD program at UCSD, which led to me joining the Trejo Lab. Dr. JoAnn Trejo has always been a great inspiration to me, and I thank her for being such a great role model for all minority students in science. If it wasn't for her great mentorship and career advice, I would not be pursuing a career in academia. I also want to thank Dr. Trejo for always checking in with me, even after graduating from UCSD and moving on to graduate school. Within the Trejo Lab, I had the pleasure of working with one of the best scientists in academia, Dr. Michael Dores. Without Dr. Dores' mentorship and career advice, I would not know how to run a protein gel or do western blotting haha. On a serious note, Dr. Dores has left a big impression on my life, that I want to be exactly the scientist he is. Everyone else in the Trejo lab was very helpful and made an impact in my choice to pursue a career in science.

Third, I joined the lab of Dr. Carrie Partch as a postbac scholar after graduating from UCSD back in 2015. Obtaining this position would not be possible without Dr. DeMaio, from UCSD, and Yulianna Ortega, Director of the UCSC STEM Diversity programs, vouching for me. I thank them both very much for the postbac opportunity. I thank Dr. Carrie Partch for the opportunity to conduct research in her laboratory. During this time, I was dealing with anxiety and stress, so I admit that I was not as

productive as I should have been. I want to thank Carrie for giving me that "talk", along with Yulianna Ortega. That "talk" motivated me to do better and led me to be a great mentor to my undergraduate mentee Ivette Perez. It helped me become motivated for graduate school at UCSC. Within the Partch Lab, I also want to thank Dr. Alicia Michael and Dr. Jenny Fribourgh for their amazing mentorship. Carrie, Alicia, Ivette, and Jenny are the definition of amazing women scientists in academia.

Fourth, I would like to thank my graduate school cohort for the support system, especially Dr. Jessie Suzuki, Dr. Apple Vollmers, Dr. Anna Russo, Dr. Guin Ashley and Dr. Londen Johnson. During graduate school, I applied for a lot of fellowships, which included a lot of writing. I want to thank Dr. Zia Isola for all the writing support during my postbac and graduate school years at UCSC. In addition, I want to thank Yulianna Ortega, Xingci Situ, and Daniela Banuelos for all their support and mentorship. Without these three women, a lot of us in the minority community would not be able to get through graduate school and our research duties. I personally would like to thank Yulianna Ortega for being an excellent advocate for promoting diversity in STEM. Another set of great mentors I would like to thank is Dr. Melissa Jurica and Dr. Seth Rubin for their scientific and career advice.

Fifth, I ended up joining the Dr. Doug Kellogg Lab for my graduate studies. Dr. Doug Kellogg has been an excellent mentor and colleague for the last 6 years or so. I want to thank Doug for being patient and allowing me to pursue my interest in conducting a thesis project that is heavy in biochemistry. He knows how much I love biochemistry and I thank him for sharing that passion with me. I also want to thank

Doug for being considerate of the personal and medical struggles I have been through during my time in his lab. I can't wait one day to call Doug one of my faculty colleagues in the future. I will always call him for advice on Biochemistry. Within the Kellogg Lab, I have made great friends with Dr. Amanda Brambila, who is now a postdoc at UCSD. Amanda is my best friend, and I will always cherish the motivation she always provided when I was at my lowest in life. Honestly, she is a big reason why I am still motivated to pursue a career in science. I would also like to thank Amanda for being like an aunt to my daughter Isabel. Dr. Tyler DeWitt and his partner Sergio Estrella have been incredible friends, and I also want to thank them from the bottom of my heart for looking out for my daughter when I was busy with research duties. They are and will always be uncles to my daughter. I want to thank two incredible scientists, David Sanchez Godinez and Francisco Solano, whom I have had the pleasure of mentoring. Thank you very much for allowing me to make a difference in your lives. I also thank David and Francisco for making me a better scientist and teacher in the lab setting. Other folks, including Beth Prichard, Dr. Maria Alcaide, Dr. Rafael Lucena, Dr. Robert Sommer, Dr. Akshi Jasani, CJ Sarabia, Selene Banuelos, Navid, Mikey, Ari, and Dr. Rafa Talavera are all incredible scientists and I thank them for their support during my time in the Kellogg Lab. If I missed anyone in the Kellogg Lab, I am very sorry, but thank you very much for any help or advice given.

Sixth, I would like to thank my extended family. I would like to thank my aunt Uyenit, my grandmother Amparo, my uncle Sergio, my cousins Sergito, Valeria, and David for providing food and shelter when my parents were deported to Mexico back

in 2007. I love them all very much. I would also like to thank my aunt Marissa and uncle Juan for all their support and love while I transitioned from high school to college. In addition, thank you to my grandmother Victoria for being very supportive throughout my life. I miss you very much. Your death still hurts me to this day. For everyone else in my extended family, I love you all very much and thank you for looking out for me throughout my life.

Seventh, I would like to thank my immediate family. Especially my mother Sonia and my father Francisco for the sacrifices they have made to give me the best life they can give their son. I know that you both struggled during the early years of my life, from not having enough money to feed yourselves, yet you provided me with food and shelter. You both did the best you could to raise me. I love you both and thank you for that. Thank you for shaping me as the well-rounded person I am today. My sister Claudia is one of my best friends in life and I love her so much. Thank you for supporting me. I also want to give a shout out to my brother Johnny and younger sister Biridiana. I love you all very much. There is a lot more I can write here about this group of amazing people, but I will just start crying haha. They know how much I love them.

Finally, I would like to thank the two loves of my life. My wife Araceli and my daughter Isabel. They are my treasures in life. Thank you very much to both of you for being part of my life and for taking care of me when I have been depressed, and when I have dealt with health problems. I would not be here without you both. I promise to provide and give you all the best life can offer when I make it to the top in academia. I love you both very much with all my heart. I also want to thank this opportunity to

thank my wife's side of the family for bringing such a beautiful and supportive women to life. For anyone that I missed, thank you very much for all the support.

Note to reader: Yeast genes are capitalized, while yeast protein names are lowercased, except for the first letter. (e.g., GIN4 (gene name) and Gin4 (protein name)).

Chapter 1: Introduction

Regulation of cell growth and size

The molecular mechanisms that explain how cells control their own size and growth is a fundamental concept of biology that is yet to be fully understood. From an evolutionary perspective, cells from earlier eukaryotes and other ancient organisms would have had to make up regulatory mechanisms that control their own growth and size to give off the unique functions of these cells that exist today. As an example of how cell size and growth play a role in cellular function, imagine the liver. If we were to digest liver tissue into individual cells and visualize these cells under a light microscope, we would observe size and shape homogeneity among the population of liver cells. This observation would suggest that cell size uniformity and proper growth are required for cellular functions (Ginzberg 2015). Therefore, cells require some form of mechanism to measure their own size. Cell size regulation and growth occur at key transition checkpoints within the cell cycle of eukaryotic cells. Two models that explain how eukaryotic cells regulate and obtain their size prior to a cell division are the sizer and adder models. In the sizer model, cells need to reach a certain size threshold prior to key cell cycle transition checkpoints regardless of their birth size from previous cell division cycles (Facchetti 2017, Soifer 2016). A model that follows the sizer mechanism is a budding yeast concentration-based mechanism of key cell cycle effectors in the G1 phase of the cell cycle. In that mechanism, it is believed that a cell cycle inhibitor called Whi5 is diluted as a yeast mother cell increases their size, which then allows a key early G1 cyclin called Cln3 to increase in concentration and promote cell cycle entry once the yeast mother cell has met a

size threshold (Schmoller 2015). In the adder mechanism, the same amount of growth in the form of biomass is added to all cells to obtain the same size prior to key cell cycle transition checkpoints and cell division (Campos 2014, Facchetti 2017). However, there is lack of evidence that suggests that the sizer mechanism is the way cells regulate and obtain a unique cell size as required to complete a full division cycle. Instead, there is greater evidence that suggests that regulation of cell size is explained by the adder mechanism. Therefore, we interpret cell size as the outcome of all mechanisms that regulate cell growth.

Growth-dependent signaling hypothesis

Previous work in the Kellogg lab leads us to believe that cells must meet a growth requirement at the G1/S (Sommer 2021) and G2/M transition checkpoints of the cell cycle (Harvey 2003, Anastasia 2012). In other words, cells must undergo a set addition of growth prior to transitioning phases within the cell cycle. Therefore, cells must have a unique way or mechanism of measuring the extent of growth to determine when sufficient growth has been met. In budding yeast, the mother cell undergoes some addition of growth via isotropic growth in the G1 phase, which means growth is added uniformly across the mother cell's surface. Once the mother cell reaches a growth threshold, the mother is ready to commit to a full division cycle and transitions into the S phase, where budding begins. The newly born daughter bud undergoes polarized growth, while the mother cell halts growth. Just like the mother cell in G1, the daughter cell undergoes growth in G2 phase until it reaches its required amount to transition into the mitotic phase. These modes of growth regulation occur

until the end of a division cycle and the daughter obtains a unique size. The budding yeast cell cycle is summarized in figure A.

How do cells measure growth? A model that explains the adder mechanism is the growth-dependent signaling hypothesis, which could explain the molecular mechanisms cells utilize to measure the extent and added amount of growth during a cell cycle event. This hypothesis states that in response to cell growth, a signal, both proportional and dependent upon growth, accumulate and that these signals behave as a readout of the extent of growth (Anastasia 2012). These "signals" that we speak of are referred to as proteins undergoing a molecular event, such as a protein undergoing phosphorylation, increasing in

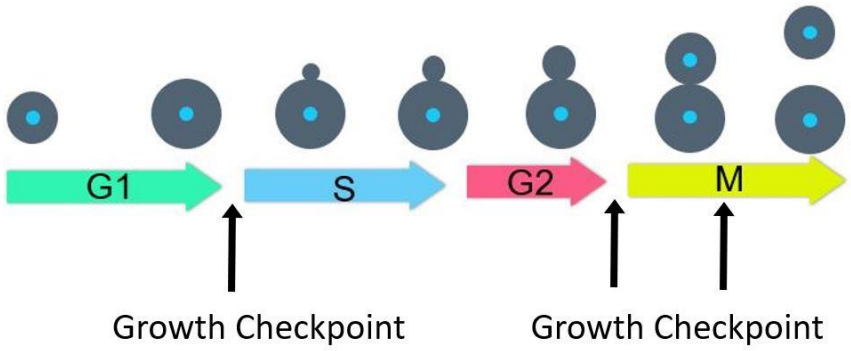

Figure A. Schematic of the budding yeast cell cycle. Shown above is a summary of budding yeast cells undergoing division. Briefly, the mother cell in G1 phase undergoes partial growth, then stops undergoing growth, while it commits to cell division by entering S phase. At this point the daughter cell initiates growth until the end of mitosis, completing division. At G1/S, G2/M, and Metaphase to Anaphase labeled by growth checkpoint arrows, cells ensure they have grown sufficient to undergo cell cycle progression.

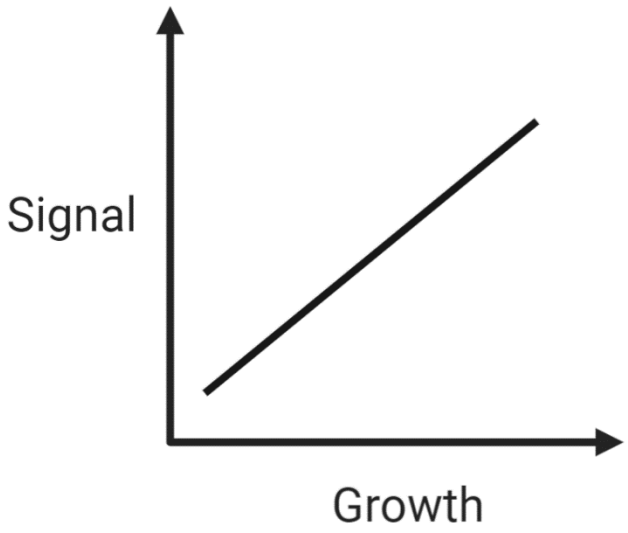

Figure B. Schematic of the growth-dependent signaling hypothesis. Shown above is a representation depicting the relationship between growth-dependent signals and membrane growth. Growth drives these signals in a proportional manner. As a signal increases in response to membrane growth, it provides a readout of the extent of growth.

The growth dependent signaling hypothesis is summarized in figure B. For example, at early G1, the cyclin Cln3 accumulates in protein levels in response to growth of the mother cell, making it a suitable candidate for functioning as a growth sensor in G1, allowing cells to read Cln3 protein levels as a measurement of the extent and added amount of isotropic growth in G1 (Sommer 2021). That is, the more growth that is added in G1, the higher the concentration of Cln3 is, giving rise to a signal that could provide when cells have met a growth threshold and therefore allows cells to initiate a cell division cycle event. Cln3 growth-dependent signaling has been shown to also be

dependent upon earlier stages of membrane trafficking and Ypk1 kinase activity, which is regulated by the TORC2 complex, known to be involved in cell growth regulation (Schmelzle 2000, Sommer 2021). Further in the cell cycle, the daughter cell undergoes polarized growth in G2, therefore, cells must also measure the extent of that growth to determine when it has met a threshold and can enter mitosis. The ideal candidate for generating growth-dependent signals is protein kinase C (Pkc1), which undergoes phosphorylation that is both dependent upon and proportional to growth in G2 (Anastasia 2012). That is, the higher the amount of growth added in G2, the more phosphorylated Pkc1 is, providing a readout of the extent of growth in G2. Once Pkc1 reaches a hyperphosphorylated state and growth threshold, it triggers biochemical events via PP2A-Cdc55-Zds1 leading to miotic entry (Anastasia 2012). As described above, the Kellogg lab has done extensive work to discover growth-dependent signals that may provide tools for cells to measure growth in G1 and G2 phases of the cell cycle. However, one key remaining question to be answered is: How do cells measure growth in mitosis?

The Gin4 kinase as a growth sensor in mitosis

In my thesis work, I studied the Gin4 kinase, which we believe is an ideal candidate for generating growth-dependent signals, serving as a growth sensor in mitosis (Jasani 2020). The Gin4 kinase is made up of two key protein domains: A kinase domain at its N-terminal region, which happens to be the ATP-binding region and the region where Gin4 binds downstream substrates and phosphorylates them. The second key domain is called the KA1-domain, which happens to be an anionic-

phospholipid binding site, especially for phosphatidylserine (PS). Binding at the KA1 domain by PS promotes localization of the Gin4 kinase to the cytosolic side of the bud neck between the mother and daughter yeast cells (Jasani 2020). In terms of the signal that Gin4 generates in response to growth, it is known that the kinase undergoes hyperphosphorylation that is dependent upon and proportional to the added growth in mitosis (Altman 1997). Thus, it is believed that Gin4 phosphorylation signals are a readout of the extent of growth, specifically in metaphase of the mitotic phase. Therefore, the more growth that occurs in metaphase, the more phosphorylated Gin4 is. It is believed that once Gin4 reaches a hyperphosphorylated state, the kinase becomes fully active and promotes inhibition of the mitotic inhibitor called Swe1 by direct phosphorylation, allowing cells to transition from metaphase to anaphase (Coleman 1993, Kanoh and Russell 1998, Opalko 2019, and Jasani 2020). How the Gin4 kinase is hyperphosphorylated and activated in mitosis is my specific thesis question. There are mammalian kinases known as MARK/PARK kinases that have similar domain architecture to Gin4, which could provide insight in its activation mechanism (Marx 2010). According to the MARK activation model, MARK kinases initially exist in an autoinhibited, closed conformation because of the kinase domain and KA1 domains interacting with each other rendering the kinases inactive (Nesic 2010, Emptage 2017). To activate the kinases, MARK must undergo structural changes in its conformation to become an open state, making it active. The current model for how MARK kinases undergo a change from closed to open states is explained by phosphorylation at the kinase domain by the Lkb1 kinase (Elm1 in

yeast) and anionic phospholipid binding, mainly PS, at its KA1 domain (Moravcevic 2010, Emptage 2018). Both biochemical events are said to be the two key steps in reversing MARK kinase autoinhibition. The Gin4 kinase may undergo similar mechanisms to undergo gradual increase in phosphorylation and activation in mitosis. In fact, it has been previously shown that Hsl1, a redundant paralog of Gin4, undergoes autoinhibition in a similar manner, except additional binding by the septins is required for Hsl1 activation (Hanrahan 2003). Previously, it was determined that the presence of Cla1, Elm1, Septins, Nap1 and among other proteins are required, genetically, for Gin4 hyperphosphorylation *in vivo* (Mortensen 2002). In addition, YCK1 and YCK2 genes, both encoding yeast casein protein kinases have also been shown to interact with the GIN4 gene, genetically. It was later discovered that Gin4 requires binding of anionic phospholipids like phosphatidylserine (PS) to undergo hyperphosphorylation as seen when the KA1, a PS-binding domain, of Gin4 is deleted (Jasani 2020). Interestingly, it is known that PS is delivered to the site of bud growth via secretory vesicles. Yck1 and Yck2 kinases also happen to be delivered to the site where the Gin4 kinase is localized during growth via membrane trafficking (Buba 1993). Further evidence suggesting that Gin4 is a growth sensor is a gin4 null mutant cell size phenotype. That is, if we deplete yeast cells of the GIN4 gene, it results in cells with an elongated bud phenotype (Altman 1997). The elongated bud phenotype suggests that cells can no longer sense and report on the extent of growth, leading to uncontrollable growth we see in these gin4Δ cells. Based on previous *in vivo* data showing requirements for Gin4 hyperphosphorylation and the Gin4 null-

mutant phenotype suggest that Gin4 acts as a growth sensor by undergoing phosphorylation in response to delivery of PS lipids to the site of growth. The Gin4 phosphorylation signals may report on the extent of growth in metaphase. In fact, a kinase dead Gin4 yeast strain also results in an elongated bud phenotype. To test if phosphorylation of Gin4 is indeed a readout of the extent of growth, we would need to map out the phosphorylation sites and mutate those sites to obtain a cell size phenotype. If Gin4 acts as a growth sensor, we would expect to get an elongated bud phenotype in a Gin4 phospho-mutant yeast strain. For my thesis work, I used genetic, biochemical, and structural biology approaches to determine the *in vitro* conditions that drive Gin4 hyperphosphorylation and activation. By determining the mechanisms by which Gin4 undergoes phosphorylation, we will gain insight on the mechanisms used to measure the extent of growth in metaphase of the mitotic phase of the cell cycle.

Importance of studying cell growth

Why is it so important to study cell growth? Imagine that we isolate cervical epithelial cells from a pap smear, and we visualize these cells under a light microscope. The cervical epithelial cells would be similar in size and the nuclear-to-cytoplasm ratio of all cells would be almost the same. However, imagine if the patient developed cervical cancer. If the same pap smear were conducted over time and cells were imaged under a light microscope, we would see drastic morphological changes compared to healthy cervical epithelial cells. The phenotype would include cells in different sizes and shapes, in addition to a larger nucleus. We interpret these results as

these cells having size and growth defects, which are nearly hallmarks of cancer. However, this phenotype is not necessarily observed in all cancer types, and we are not sure if these cell defects are a cause or consequence of cancer. Therefore, cell size and growth control could play a regulatory role in cancer. One of our applicable goals is to determine the mechanisms that control and measure cell growth in healthy cells using budding yeast as our model of study, because of the high genomic similarity to human cells. Once we know the mechanisms that control cell growth and size in yeast, we would like to determine how these mechanisms are disrupted in cancer cells in the hope of developing therapeutic targets.

Chapter 2: Molecular mechanisms of growth-dependent activation of the Gin4 kinase (Modified writing version of manuscript to be submitted for publication)

Introduction

Cells must grow sufficiently to meet a unique size threshold prior to cell division. How cells determine when sufficient growth has been met prior to cell division is a fundamental question of cell biology that remains to be fully understood. Since cells need to track the amount of growth added within a cell cycle event, there must be a mechanism or mechanisms that cells use to measure the extent of growth. A model that explains how cells measure the extent of added membrane growth during the cell cycle is the growth-dependent signaling hypothesis. In such hypothesis, it is predicted that as cells undergo membrane growth, there is a signal that accumulates proportionally to and dependent upon growth (Anastasia 2012). These "signals" are referred to as proteins undergoing molecular events such as protein phosphorylation, changes in protein levels, and among other biochemical events in a growth-dependent manner, and in a way where the signals that arise from the molecular events gradually increases until sufficient growth has been reached by the cell. We also refer to these signals as potential "growth sensors" because their activity in response to cell growth could provide a readout of the extent of growth within a certain period or phase of the cell cycle. A key step towards testing this hypothesis is to define the molecular mechanisms that drive growth-dependent phosphorylation of Gin4 in mitosis. In this work, we are interested in determining the molecular mechanisms that drive

phosphorylation and activation of the Gin4 kinase, a potential growth sensor, that could provide information on the extent of growth in metaphase of the mitotic phase.

Previous studies demonstrated that the Gin4 kinase undergoes hyperphosphorylation that is both proportional to and dependent upon membrane growth (Jasani 2020). Therefore, Gin4 phosphorylation signals could behave as a readout of the extent of growth in metaphase, especially since majority of cell growth occurs in mitosis for yeast cells. Additional evidence that supports Gin4 as a growth sensor are cell size phenotypes of null gin4 and kinase dead (K48A) Gin4 mutants (Jasani 2020). Both mutants result in elongated bud phenotypes, suggesting that these mutants can no longer detect the correct type and amount of growth. In other words, these Gin4 mutants lose their "growth sensing" function. In addition, these phosphorylation events have been shown to correlate with Gin4 kinase activity, therefore, suggesting that hyperphosphorylation of Gin4 activates the kinase for downstream activity in mitosis (Altman 1997).

It is believed that once Gin4 reaches a hyperphosphorylated state, the kinase becomes fully active and promotes inhibition of the mitotic inhibitor called Swe1, allowing cells to transition from metaphase to anaphase (Jasani 2020). How these Gin4 phosphorylation signals are generated is the key question of this work. Previous *in vivo* studies have determined that Gin4 phosphorylation events are dependent upon lipid binding events at its KA1 C-terminal domain by binding phosphatidylserine (PS) (Jasani 2020) and requires Elm1 kinase activity (Screenivasan 1999), both which fit into previous models of activation of MARK/PARK kinases, which are

homologous to Gin4 in its domain architecture (Nesic 2010, Emptage 2017). Elm1 has been previously determined to directly phosphorylate Gin4 at the flexible linker region between the kinase domain and KA1 domains, however, from that study (Asano 2006), it is not clear if Elm1 is sufficient to drive full hyperphosphorylation of Gin4. Other *in vivo* studies have determined that the kinase Cla4 is required for Gin4 hyperphosphorylation (Tjandra 1998), however, Cla4 is known to be required for determining the site of bud growth, which could contribute to Gin4 phosphorylation by promoting proper bud growth. Lastly, the nucleosome assembly protein-1, Nap1, protein is required for Gin4 phosphorylation *in vivo* (Altman 1997). Nap1 is also required for normal mitotic progression by the mitotic cyclin Clb2 (Kellogg and Murray 1995), suggesting the Gin4 activation and its role in mitotic progression is dependent on Nap1 and Clb2 proteins.

All previous candidates determined to be genetically required for Gin4 hyperphosphorylation *in vivo*, are also required for Swe1 hyperphosphorylation and degradation. Two major candidates for promoting growth-dependent phosphorylation of Gin4 *in vivo* are phosphatidylserine and the yeast casein kinases 1/2. PS is delivered to the site of bud growth on secretory vesicles via exocytosis, promoting binding and localization of Gin4 to the bud neck. In this manuscript, we identify a new genetic interaction between YCK1, a yeast casein kinase, and GIN4. Yck1 is a palmitoylated kinase that is transported to the site of growth via secretory vesicles in response to membrane growth (Babu 2002), like the delivery of PS lipid to the bud neck. yck1Δ yck2 temperature sensitive yeast mutants display an elongated bud

phenotype, like a gin4Δ phenotype, suggesting that Yck1/2 and Gin4 work in a similar pathway to control mitotic progression (Robinson Et al. 1993). Lastly, yck1Δ yck2 temperature sensitive yeast mutants lead to a mitotic arrest with high levels of Cdk1 inhibitory phosphorylation, suggesting Yck1/2 kinases are required for proper mitotic progression. Interestingly, Casein kinase 2 in Drosophila directly phosphorylates Nap1, which could explain the positive genetic relationship between YCK1/2 and NAP1 genes (Li 1999). We hypothesize that Yck1 may be a direct regulator of Gin4, in addition to Elm1, by localizing to the bud neck, where it is positioned near Gin4 for biochemical activity. With all these *in vivo* requirements known, it is not clear how all these factors work to promote Gin4 phosphorylation and activation *in vitro*. In this work, we demonstrate the development of an MBP-8xHis tagging system to generate yeast strains in which we can purify from tagged forms of Gin4, Elm1, and Yck1 proteins to generate *in vitro* reconstitution systems in varying conditions, including the presence of PS-containing liposomes to determine the direct biochemical mechanisms of Gin4 hyperphosphorylation.

Results

Development of MBP-8xHis tag purification system of yeast proteins for Gin4 *in vitro* kinase assays

To test different models of Gin4 hyperphosphorylation and activation *in vitro*, a two-step affinity chromatography purification protocol was developed to readily purify C-terminally MBP-8xHis tagged yeast proteins and protein complexes. To generate yeast strains harboring C-terminally tagged proteins, we relied on a one-step PCR-mediated homologous recombination of yeast genome developed by Mark. S. Longtine (Longtine 1998 et al.). We modified the original longtine plasmid containing a GST tag sequence with a HIS nutritional marker gene (pFA6a-GST-HIS3MX6) by replacing the GST gene with a yeast codon-optimized MBP-8xHIS gene by traditional restriction digest and ligation molecular cloning techniques. To C-terminally tag yeast proteins, we transformed PCR-amplified gene products made up of the MBP-8xHis gene with a TEV recognition site upstream the double tag with 5' and 3' flanking regions homologous to gene to be tagged. To purify proteins for Gin4 *in vitro* kinase assays, we followed a two-step purification system: 1) A nickel chromatography step, which is used to bind His-tagged proteins followed by a 2) amylose chromatography step, which is used to bind the MBP-tagged proteins. Following this general protocol, we can obtain reasonable amounts of protein ranging from 16 to 400 μg in yield, depending on the protein, for in-solution *in vitro* kinase assays. As an example, an MBP-8xHis tagged Gin4 kinase can be purified to high purity in complex with Nap1 from log-phase yeast cells (Figure 1). Previous co-immunoprecipitation studies have

determined that Gin4 binds to Nap1 throughout the cell cycle at a high affinity, since high amount of salt is required to break up a Gin4-Nap1 interaction (Altman 1997).

Binding to phosphatidylserine is not sufficient to induce Gin4 phosphorylation *in vitro*

Phosphatidylserine (PS) is an anionic phospholipid thought to bind Gin4 at its N-terminal KA1 domain (Moravcevic 2010). Deleting the KA1 domain results in Gin4 no longer localizing to the bud neck and failure of Gin4 to undergo hyperphosphorylation *in vivo* (Jasani 2020). Therefore, we propose a direct mechanism in which PS is delivered to the bud neck via secretory vesicles and bind Gin4 to induce autophosphorylation of the kinase. To do so, we performed an *in vitro* kinase assay with increasing molar percentage amounts of PS incorporated into prepared liposomes in the presence of purified Gin4. Gin4 on its own underwent partial autophosphorylation in the presence of ATP, however, increasing amounts of PS lipid did not induce further Gin4 autophosphorylation (Figure 2). These *in vitro* observations suggest that Gin4 can undergo minimal autophosphorylation on its own and PS lipid binding at the KA1 domain is not sufficient to drive Gin4 phosphorylation *in vitro*. Therefore, we next tested a kinase driven Gin4 hyperphosphorylation model.

Elm1 directly stimulates Gin4 autophosphorylation *in vitro*

Multiple kinase candidates are required for Gin4 hyperphosphorylation *in vivo*, including the Cla4 and Elm1 kinases. Cla4 is likely to indirectly drive Gin4 hyperphosphorylation by playing a role in marking the site for bud growth, therefore, not likely to regulate Gin4 phosphorylation directly (Tjandra 1998). The Elm1 kinase

is homologous to the mammalian Lkb1 kinase, which is implicated to activate MARK kinases that have similar domain structure to Gin4 (Nesic 2010, Emptage 2017). Therefore, we next determined if Elm1 can directly phosphorylate Gin4 *in vitro*. Introduction of increasing amounts of purified Elm1 (Figure 3A) induced Gin4 hyperphosphorylation *in vivo* as indicated by the increased electrophoretic mobility gel shift (Figure 3B). Similar results were previously determined by radioactive P^{32} incorporation of Gin4 in the presence of Elm1 on immobile beads (Asano 2006). The key difference in our work is assaying Gin4 phosphorylation by changes in electrophoretic mobility gel shifts in free solution. By assaying for Gin4 phosphorylation via mobility gel shift gives us the advantage to measure Gin4 phosphorylation directly, compared to the shifts we observe *in vivo*. Radioactive P^{32} incorporation kinase assays won't allow us to visually look at a Gin4 phosphorylation shift, however, radioactivity can help determine phosphorylation events that may not necessarily result in a gel mobility shift. Next, we asked if *in vitro* Elm1-dependent phosphorylation of Gin4 is due to direct phosphorylation by Elm1 or stimulated Gin4 autophosphorylation by Elm1. Therefore, we used a purified, kinase dead version (K48A) of Gin4 as a substrate. Elm1 failed to phosphorylate kinase dead Gin4 *in vitro* compared to wild type Gin4 (Figure 3C), suggesting Elm1 stimulates Gin4 autophosphorylation *in vitro*. Although, it was previously determined that Elm1 can phosphorylate kinase dead Gin4 by radioactive P^{32} incorporation (Asano 2006), suggesting that Elm1 may phosphorylate Gin4 directly at multiple sites to stimulate further Gin4 autophosphorylation. Furthermore, we figured that addition of PS lipid

could induce conformational change on Gin4 to make it a better substrate for Elm1; therefore, we also tested if addition of PS-containing liposomes induced further Gin4 autophosphorylation. We observed no changes in Elm1-dependent Gin4 phosphorylation *in vitro* (Figure 3D). Therefore, Elm1-dependent Gin4 autophosphorylation is not dependent on PS lipid *in vitro*.

Yck1/2 kinase activity is required for Gin4 hyperphosphorylation

Since we needed molar excess of Elm1 to observe Gin4 hyperphosphorylation, we reasoned that it may be due to a partially active Elm1. Furthermore, we hypothesized that an additional kinase may act on Gin4 and/or Elm1 kinase activity is stimulated by an upstream kinase to act on Gin4. The ideal candidate for promoting Gin4 phosphorylation in these possible scenarios is the Yck1 kinase, due to its localization to the bud neck influenced by the processes of cell growth (Babu 2002). In addition, inactivation of Yck1/2 kinases results in an elongated bud phenotype like elm1 and gin4 null mutants (Altman 1997, Screenivasan 1999, Jasani 2020), suggesting all these kinases work in the same signaling pathway. We first tested whether Yck1/2 plays a role in growth-dependent phosphorylation of Gin4. To do this, we utilized an analog-sensitive allele of *YCK2* in an *yck1*Δ background (*yck2-as yck1*Δ), which allowed rapid and specific inhibition of Yck1/2 activity with the adenine analog 3-MOB-PP1 (Credit to Steph Anastasia, Maria Alcaide, and Akshi Jasani; work not published). Wild type control cells and yck2-as yck1Δ cells were released from a G1 arrest and analog inhibitor was added to both cultures at 15 minutes after release. Hyperphosphorylation of Gin4 was assayed via western blot to detect electrophoretic

mobility shifts caused by phosphorylation. We also assayed levels of the mitotic cyclin Clb2 as a marker for mitotic progression. Gin4 failed to undergo hyperphosphorylation when Yck1/2 were inhibited compared to wild type cells (Figure 4A), and the cells arrested in mitosis (Figure 4B). Since activation of Gin4 is thought to lead to hyperphosphorylation and inhibition of Swe1 (Jasani 2020), we also assayed Swe1-dependent inhibitory phosphorylation with a phosphospecific antibody that detects phosphorylation of Cdk1 on tyrosine 19. This showed that inhibition of Yck1/2 also leads to an arrest with high levels of Cdk1 inhibitory phosphorylation (Figure 4C).

Delays in Clb2 protein levels and inhibitory Cdc28 Y19 phosphorylation levels by inactivation of Yck1 and Yck2 kinase activity using a temperature sensitive strain were previously reported (Pal Et al. 2008). Here we show similar observations using an analog sensitive Yck2 mutant strain. These observations suggest that Yck1/2 kinase activity is required for full hyperphosphorylation of the Gin4 kinase in response to mitotic growth and required for normal mitotic progression. Therefore, it is possible that the Gin4 kinase could be directly interacting with and phosphorylated by the Yck1/2 kinases at the bud neck in yeast.

Localization of Yck1/2 to the plasma membrane is required for Gin4 hyperphosphorylation and normal mitotic progression

Yck1/2 are anchored to the plasma membrane via a C-terminal palmitoyl group, which is added by a palmitoyl transferase named Akr1 (Feng Y 2002, Roth 2002, Babu 2004, and Pasula 2010). Loss of Akr1 causes loss of plasma membrane localization of Yck1/2, as well as defects in control of cell growth However, loss of Akr1 is not lethal,

whereas loss of Yck1/2 is lethal, which suggests that Yck1/2 have functions that are not dependent upon their localization to the plasma membrane (Feng Y 2002, Roth 2002, Babu 2004, and Pasula 2010). To test whether localization of Yck1/2 to the plasma membrane is required for their role in driving Gin4 hyperphosphorylation, we analyzed Gin4 hyperphosphorylation in *akr1*Δ cells. Wild type and akr1Δ cells were released from a G1 arrest and Gin4 hyperphosphorylation was assayed by western blot. Hyperphosphorylation of Gin4 failed to occur normally in akr1Δ cells compared to wild type cells (Figure 5A) and resulted in a mitotic delay (Figure 5B). Although, we still observed some Gin4 phosphorylation in akr1Δ cells, supporting the idea that Yck1/2 may be able to function independently to some extent without localizing to the membrane. In addition, inhibitory phosphorylation of Cdk1 was increased, as expected for a failure to activate Gin4 (Figure 5C).

These observations suggest that Yck1/2 membrane localization is required for full hyperphosphorylation of the Gin4 kinase in response to mitotic growth and required for normal mitotic progression. Therefore, the data suggest that Yck1/2 could be a strong candidate for an upstream kinase that phosphorylates Gin4 at the plasma membrane, playing a direct role in growth sensing and cell cycle progression.

Yck1 stimulates further Gin4 phosphorylation in an Elm1 dependent manner *in vitro*

Now that we have identified Yck1 as a kinase required for Gin4 hyperphosphorylation *in vivo*, we next tested if Yck1 can directly phosphorylate Gin4 and/or could stimulate further Elm1-dependent Gin4 autophosphorylation *in vitro*. To do so, we introduced purified Yck1 (Figure 6A) into our Gin4 *in vitro* assays. Yck1 on its own failed to phosphorylate Gin4 directly *in vitro*, however, Yck1 seemed to stimulate further Gin4 phosphorylation in the presence of Elm1 *in vitro* (Figure 6B). Some casein kinases are thought to undergo autoinhibition via autophosphorylation of their C-terminal tails (Graves 1995, Cegielska 1998, Budini 2009). Therefore, we reasoned that full-length Yck1 may only be partially active and that introducing a C-terminal truncated form of Yck1 (Figure 6C) may stimulate significant increase in Elm1-dependent Gin4 phosphorylation. We observed that full length Yck1 is still more effective in driving further phosphorylation of Gin4 *in vitro* compared to the truncated form of Yck1 (Figure 6D), which could be explained by the C-terminal region possibly being an important site of regulation, acting as an Elm1 and/or Gin4 binding site. Therefore, Yck1 influences Gin4 phosphorylation *in vitro* in the presence of Elm1.

Yck1 is required for hyperphosphorylation and activation of Elm1 *in vivo* and *in vitro*

The Yck1-Elm1 *in vitro* results suggest possible roles for Yck1 in driving growth-dependent phosphorylation of Gin4. First, Yck1 directly phosphorylates and activates Elm1, leading to Elm1-dependent phosphorylation of Gin4 *in vitro*. Second,

Yck1 directly phosphorylates Gin4 in an Elm1-dependent manner via a priming or template-based mechanism where Elm1 acts on Gin4 first, leading Yck1 to then act on Gin4. To test the first possibility, we first determined what constitutes an active form of Elm1 by establishing how Elm1 behaves during a cell cycle event *in vivo*. Using synchronized myc-tagged Elm1 yeast cells, we observed a steady hyperphosphorylated Elm1 throughout the cell cycle. Surprisingly, hyperphosphorylated myc-tagged Elm1 increased in levels during mitosis (Figure 7A). Therefore, we hypothesize that Elm1 becomes activated by high levels of hyperphosphorylation. Next, we asked if Yck1 plays a role in hyperphosphorylation and activation of Elm1 by tracking changes in Elm1 phosphorylation in an yck1 yck2-as background. Inactivation of Yck1/2 kinases resulted in a significant decrease in Elm1 hyperphosphorylation (Figure 7A), suggesting that Yck1/2 kinases are upstream regulators of Elm1 kinase activity *in vivo*. Next, we asked if Yck1 can directly phosphorylate Gin4 vitro. We observed phosphorylation of Elm1 in the presence of full length Yck1 as indicated by an increased in electrophoretic mobility gel shift, but not in the presence of the truncated form of Yck1 (Figure 7B), suggesting full-length Yck1 is direct regulator of Elm1 kinase activity. Although, the latter has only been confirmed by one experiment. We will need to repeat Elm1/Yck1 *in vitro* kinase assays to determine if Yck1 does directly phosphorylate Elm1 *in vitro*.

Model for growth dependent phosphorylation and activation of Gin4

Based on our genetic and biochemical analysis of growth dependent Gin4 phosphorylation, we propose a model (Figure 8) in which phosphatidylserine and Yck1/2 kinases are localized to the site of growth via secretory vesicles in response to membrane growth. Phosphatidylserine recruits the Gin4 kinase to the plasma by binding it to its C-terminal KA1 domain. Yck1 kinase is anchored to the membrane by palmitoylation at its C-terminal tail, where it promotes Elm1 phosphorylation and activation either indirectly or by direct phosphorylation. This Elm1 activation event in turn leads to direct phosphorylation and stimulation of Gin4 autophosphorylation by Elm1, leading to Gin4 activation. We cannot rule out the possibility of Yck1 acting on Gin4 in an Elm1-dependent manner. Further *in vitro* studies will be required to determine if Elm1 primes Gin4 for Yck1-dependent phosphorylation on the kinase. We propose that Gin4 phosphorylation signals report on the extent of membrane growth during metaphase of the mitotic phase. Once Gin4 reaches a hyperphosphorylated state, sufficient growth and full activation of Gin4 triggers inactivation of the mitotic inhibitor Wee1/Swe1 by hyperphosphorylation, leading to full activation of Cdk1. High activity of Cdk1 then promotes metaphase to anaphase transition, allowing cells to complete division. It remains unclear if active Gin4 directly phosphorylates Wee1/Swe1 *in vitro*, which is an experiment we plan to pursue this summer to complete the work on regulation and function of the Gin4 kinase in mitosis.

Materials and Methods

Yeast strain construction, plasmid construction, media, and reagents

All the yeast strains are in the W303 background (leu2-3, 112 ura3-1, can1-100, ade2-1, his3-11, 14 trp1-1, GAL+, ssd1-d2). Yeast cells were cultured in YP medium (yeast extract, peptone, 40 mg/L adenine) supplemented with dextrose (YPD), unless stated otherwise in specific experiments.

To generate yeast strains, deletions and c-terminal tagging of genes were carried out by standard PCR amplification and homologous recombination (Longtine et al. 1998, Janke et al. 2004). In general, all strains were constructed by the transformation of a PCR-amplified DNA fragment with 40 bp homologous arms of gene targets outside the coding region with a drug or nutritional selection marker. Specifically, The yck1Δ yck2-as strain was generated as previously described (Lucena 2023, in preparation). akr1Δ cells were generated by integrating PCR-amplified KANMX6 fragment from the pFA6a-KanMx plasmid with 40 bp flanking AKR1 homologous sequences into wild-type (BAR+) cells. MBP-8XHIS-tagged strains of GIN4, YCK1 FL, YCK ΔC, and ELM1 were generated by the integration of PCR-amplified MBP-8XHIS:HIS3MX6 fragments with 40 bp of flanking homologous sequence of each gene from the pFA6a-MBP-8XHIS-HISMX6 plasmid into wild type (bar-) cells. A TEV recognition site was engineered between the end of the gene and MBP sequence for tag cleavage by the TEV protease. In addition, an additional 6xHIS sequence was engineered at the end of YCK1 to mimic its lipid-

anchoring nature in *in vitro* kinase assays that include liposomes. To generate 9xMyc-tagged ELM1 strains, integration of PCR-amplified 9xMYC-Hygromycin fragments with 40 bp of flaking homologous ELM1 sequence were performed into wild type (bar-) and yck1Δ yck2-as cells.

Plasmids pFA6a-KanMx, pFA6a-GST-HIS3MX6 and pFA6a-HIS3MX6 were constructed as previously described (Longtine et al. 1998). The pFA6a-MBP-8xHIS-HISMX6 plasmid was constructed by restriction enzyme-based cloning. Briefly, yeast codon optimized MBP-8XHIS DNA sequence with flanking PacI and AscI restriction sites was synthesized by TWIST Biosciences, Inc. Additional fragments of MBP-8XHIS with PacI and AscI sites were amplified via PCR, then digested with AscI and PacI restriction enzymes. The pFA6a-GST-HIS3MX6 plasmid was also digested with AscI and PacI restriction enzymes to remove the GST gene. Cut MBP-8xHIS sequence was then inserted into the AscI and PacI sites of digested pFA6-HIS3MX6 via ligation. Successful ligation was confirmed via diagnostic restriction digest and sequencing (Azenta Inc.). Plasmids used to express and purify His-tagged and GST-tagged TEV protease in E. coli were gifts from the Carrie Partch and Seth Rubin labs, respectively. Protocols from the Partch and Rubin labs were used to purify TEV proteases.

Yeast extract and peptone powder were purchased from BP Diagonistics. Adenine hemisulfate salt was purchased from Sigma Aldrich. Dextrose powders was purchased from Fischer Scientific. Glycerol (99.7%, ACS) was purchased from EMB Millipore. Ethanol (100 and 200 proof) were purchased from Gold Shield. All

restriction enzymes and amylose resin for MBP-tagged protein purifications were purchased from NEB Labs. Nickel resin for His-tagged proteins were purchased from Sigma-Aldrich. All lipids, including brain PS, egg PC, and DGS (Ni) were purchased from Avanti Polar Lipids, Inc.

Cell cycle time course experiments and western blotting

Cell cycle time course experiments were conducted as previously described (Harvey et al. 2011). Briefly, for the yck analog-sensitive experiment, wild type and yck1Δ yck2-as yeast cells were grown in YPD medium (yeast extract, peptone, and dextrose) without adenine (YPD-ADE) at room temperature for 12-16 hours until cells reached an optical density (OD_{600}) between 0.4-0.7. Wild type cells were adjusted to have an OD_{600} of 0.5 and yck1Δ yck2-as were adjusted to 0.65. Cells were synchronized at G1 phase by treating cells for 3 hours at room temperature with alpha mating factor to a final concentration of 0.5 μg/mL. Cells were released from a G1 arrest by three rounds of pelleting followed by resuspension with an equal volume of YPD-ADE medium. After the final wash, cells were transferred to 25 ◦C. Starting at 30 minutes after release from G1 arrest, 1.6 mL samples were collected every 10 minutes until a total of 150 minutes were reached. To ensure one cell cycle event was tracked, alpha factor was added at the same volume, again, at 60 minutes after G1 arrest release. Samples were processed for SDS-PAGE gel electrophoresis and western blotting by: Pelleted cells followed by removal of supernatant. Acid-washed microbeads were added to the pellet and flash-freeze in liquid nitrogen. Cells were lysed by adding 140 μL of 1x sample buffer (65 mM Tris-HCl pH 6.8, 3% SDS, 10%

glycerol, 5% beta-mercapethanol, and bromophenol blue) supplemented with 2 mM PMSF and placed in a mini-beadbeater 16 (BioSpec) at top speed for 2 minutes at 4 ◦C. After, samples were centrifuged followed by boiling at 95 C for 5 minutes, then, centrifuged again for 5 minutes at 15,000 rpm using a table-top microcentrifuge. Protein samples (10 µL) were separated by passing 20 mA of current through a 10% polyacrylamide gel submerged in running buffer (Glycine, Tris base, 10% SDS), then transferred to a nitrocellulose membrane at 4 ◦C using a wet transfer apparatus at 800 mA in 1x transfer buffer (Tris base, glycine, and methanol) when probing for Gin4 or using a semi-dry turbo blotter (BioRad) when probing for Clb2, Nap1, and Cdc28 Y19 P. Blots were probed with primary antibody at 1-2 ug/mL overnight at 4 ◦C in 5% milk in PBST (1x phosphate-buffered saline, 250 mM NaCl, and 0.1% Tween-20) containing 5% nonfat dry milk. Primary antibodies to detect Gin4, Nap1, and Clb2 were rabbit polyclonal antibodies generated as described previously (Kellogg and Murray 1995, Screenivasan and Kellogg 1999, Mortensen et al. 2002). Phosphorylated Cdc28 at tyrosine 19 was detected using a Cdc2 Y15 monoclonal primary antibody (Cell Signaling Inc.). Primary antibodies were detected by using an HRP-conjugated donkey anti-rabbit secondary antibody (for Gin4, Nap1, and Clb2) or HRP-conjugated donkey anti-mouse secondary antibody (Cdc28 Y19 P) incubated in 5% milk PBST solution for 1 hour at room temperature. Blots were rinsed in 1x PBST, followed by a final wash in 1x PBS before detection via chemiluminescence using ECL reagents with a Bio-rad ChemiDoc imaging system.

For the akr1Δ experiments, wild type and akr1Δ yeast cells were grown in YPD supplemented with adenine (40 mg/L) to similar optical density conditions as described above. Since these cells are Bar+ strains, cells were synchronized by adding alpha mating factor was added to a final concentration of 15 ug/mL. Cell samples were collected and processed for western blotting analysis as described above.

For the Elm1-9xMyc time course experiments, the protocol for the yck1Δ yck2-as experiment was used here. Except the time at which samples were collected varied. Elm1-9xMyc was probed via western blotting as described above, but with the use of a Myc antibody.

Purification of MBP-8xHis tagged yeast proteins

Full length and C-terminal truncated YCK1, ELM1, and GIN4 MBP-8xHis strains were grown in 6 L of YPD media for 12-16 hours at 22 ◦C until log phase (OD_{600} 0.4-0.6) was reached. Cells were harvested by low-speed centrifugation at 5,000 rpm at 4 ◦C using the JLA 9.1000 Beckman rotor. Cell pellets were scooped out using a spatula and immediately flash-frozen in liquid nitrogen. Lysis of cells was performed by grinding frozen chunks of cells in dry ice using a coffee grinder for 30 seconds, then transferred to a pre-chilled mortar. Cell powder was further grounded using a pestle with constant addition of liquid nitrogen to keep the cells cold. Powder was then stored for 12-16 hours at -80 ◦C to allow for the evaporation of carbon dioxide. To create a cell lysate, 10-15 grams of each cell powder was resuspended in 3 volumes (3 x weight of cell powder) of ice-cold lysis buffer (50 mM HEPES-KOH

pH 7.6, 175 mM KCl, 0.5% Tween-20, 1 mM MgCl2, 1 mM EGTA, 10 mM Beta-glycerol phosphate, and 2 mM PMSF), except in the Yck1 protein purification, no Beta-glycerol phosphate was used in the lysis buffer. A supernatant with soluble protein was obtained by centrifugation of cell lysate at 20,000 RPM at 4 ◦C using the JA-20 beckman rotor. The supernatant was transferred to an ice-cold beaker and the pellet was discarded. Clarified lysate was applied to a pre-equilibrated 5 mL Nickel resin column at 20 mL/hour using a peristaltic pump at 4 C. After sample application, the column was washed with 10 column volumes of nickel washing buffer (50 mM HEPES-KOH pH 7.6, 175 mM KCl, 5 mM Imidazole, 1 mM EGTA, 1 mM DTT) at 50 mL/hour. MBP-8xHis tagged proteins were eluted from the nickel column by applying 1.5 mL fractions of nickel elution buffer (50 mM HEPES-KOH pH 7.6, 175 mM KCl, 100 mM Imidazole, 1 mM EGTA, 1 mM DTT, 10% glycerol). Elution of protein from the nickel column was tracked via Bradford assays of individual fractions, and fractions with the strongest signals were pooled. Pooled nickel eluate was then immediately applied to a 1 mL amylose resin column (pre-equilibrated with nickel elution buffer) at 10-15 mL/hour using a peristaltic pump at 4 ◦C. Amylose column was then washed with 10 column volumes of high salt MBP washing buffer (50 mM HEPES-KOH pH 7.6, 1 M KCl, 1 mM DTT, 10% glycerol), except 175 mM KCl was used for Gin4 protein purification. For Yck1 and Elm1 purifications, an additional washing step with 5 column volumes of 175 mM KCl buffer was performed to reduce salt concentration. The amylose columns were washed with 450 µL of MBP elution buffer (50 mM HEPES-KOH pH 7.6, 175 mM KCl, 1 mM DTT,

10 mM Maltose, and 10% glycerol). Proteins were eluted by applying 1 mL of the same elution buffer. Proteins were concentrated using a 30K MWCO 0.5 mL PES Pierce concentrator to a final volume of 150-200 µL. Samples were supplemented with MgCl2 to a final concentration of 1 mM and Tween-20 to a final concentration of 0.01%. Purified proteins were aliquoted, flash-frozen in liquid nitrogen, and stored at -80 ◦C for *in vitro* kinase assays.

Preparation of liposomes for *in vitro* kinase assays

Lipid suspensions of 5% DGS (Ni), 15% PS, and 80% PC (mol%) were made in low-retention microcentrifuge tubes and subjected to a low-speed centrifugation spin with heat and in vacuum to create a dry lipid film. The lipid film was washed with 50 µL of sterile water and transferred back to the vacuum-sealed centrifuge until all the water evaporated. Lipids were then resuspended in 50 mM HEPES-KOH pH 7.6, 175 mM KCl and incubated at 60 ◦C in a water bath for 30 minutes. Six freeze/thaw cycles were then performed: Sample was frozen in liquid nitrogen and thawed at 60 ◦C in a water bath for 5 minutes. Lipid suspension was then passed through an Avanti extruder pre-heated to 60 ◦C for a total of 8-10 passes. Liposomes were stored at 4 ◦C for a maximum of 5 days, until they were no longer good for use. Final concentration of liposomes was 1 mM and used at 0.5 µM final concentration in *in vitro* kinase reactions, except for the liposome titration experiment in the presence of Elm1 and Gin4 kinases, a range of 0.01-0.5 µM final liposome concentrations were used.

Gin4 *in vitro* kinase assays

All purified MBP-8xHis-tagged proteins were pre-treated with His-tagged TEV protease for 2.5 hours at 30 ◦C to remove the tags. In some experiments, MBP-8xHis-tagged proteins were pre-treated with GST-tagged TEV protease for 12-26 hours at 4 ◦C. Untagged Gin4 kinase was used at 100-200 ng in our *in vitro* assays. Purified untagged Elm1 and FL/ΔC Yck1 were used in the range of 20 ng-1000 ng, depending on the experiment. In experiments were PS-containing liposomes were used, the working concentration used was 0.5 uM. Purified Gin4 kinase was reconstituted in varying conditions with liposomes, Elm1, and FL/ΔC Yck1 in kinase assay buffer (20 mM Tris-acetate pH 7.8, 50 mM Potassium acetate, 1 mM Magnesium acetate,0.5 ug BSA, 1 mM MnCl2, and 1 mM ATP) for a final volume of 25 µL. *In vitro* reactions were incubated at 30 ◦C for 1 hour, then quenched by TCA precipitation and resuspension of protein pellets in 22 µL of 1x sample buffer (recipe described above). Gin4 phosphorylation was assayed by electrophoretic mobility gel shift via western blotting, as described above.

Figures

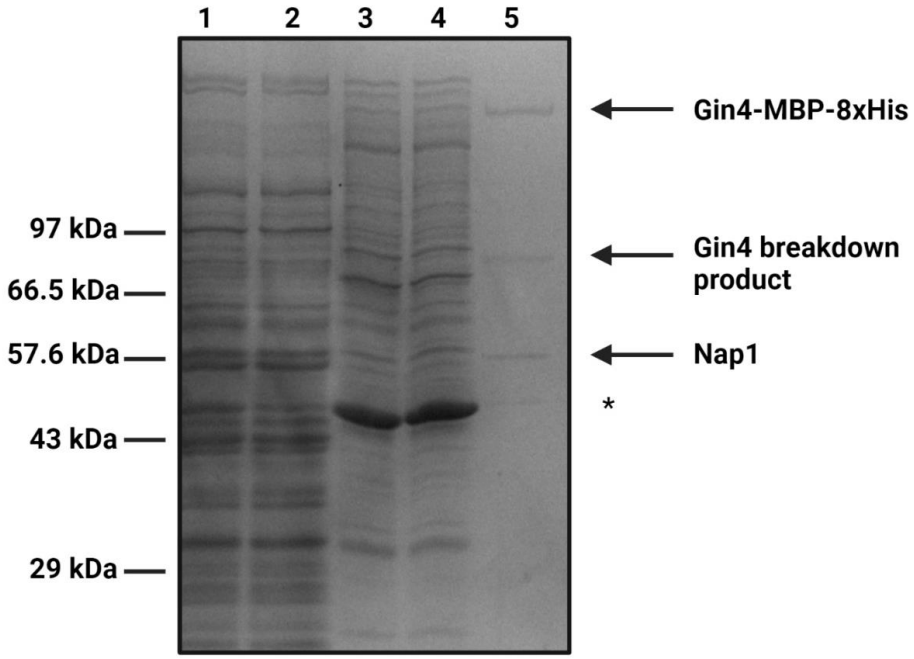

Figure 1. Coomassie-stained gel image of purified Gin4-Nap1 complex. Gin4-Nap1 complex was purified from log-phase yeast cells using a two-step chromatography process. In lane 1 is the cell extract, lane 2 is the flow-through from a nickel column, lane 3 is eluate from nickel column, lane 4 is flow through from an amylose column, and lane 5 is our final purified Gin4-Nap1 complex from an amylose column. There is a major Gin4 breakdown product below 97 kDa. The asterisk (*) denotes a contaminating protein that was not identified.

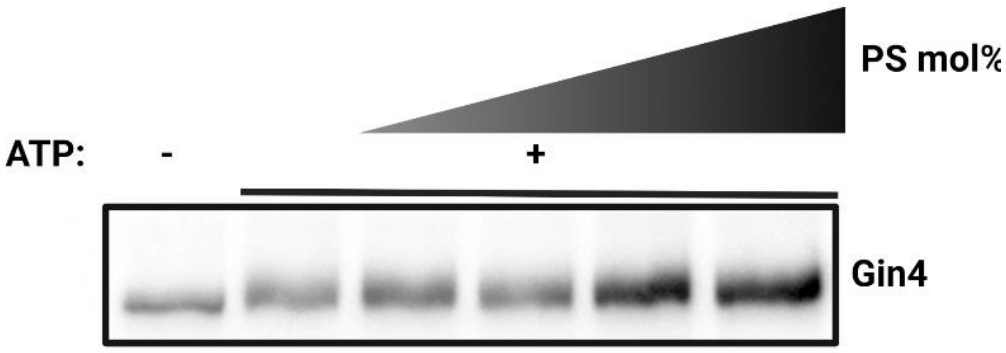

Figure 2. Phosphatidylserine binding to the KA1 domain is not sufficient to drive Gin4 hyperphosphorylation *in vitro*. Purified Gin4 kinase was incubated with ATP on its own, and in other reactions with increasing amounts of PS lipid ranging from 15%-30% (mol%) incorporated into liposomes in the presence of ATP at 30 C for 1 hour. Gin4 phosphorylation was assayed by electrophoretic mobility gel shift via western blotting. This western blot is representative of an experiment with n =3.

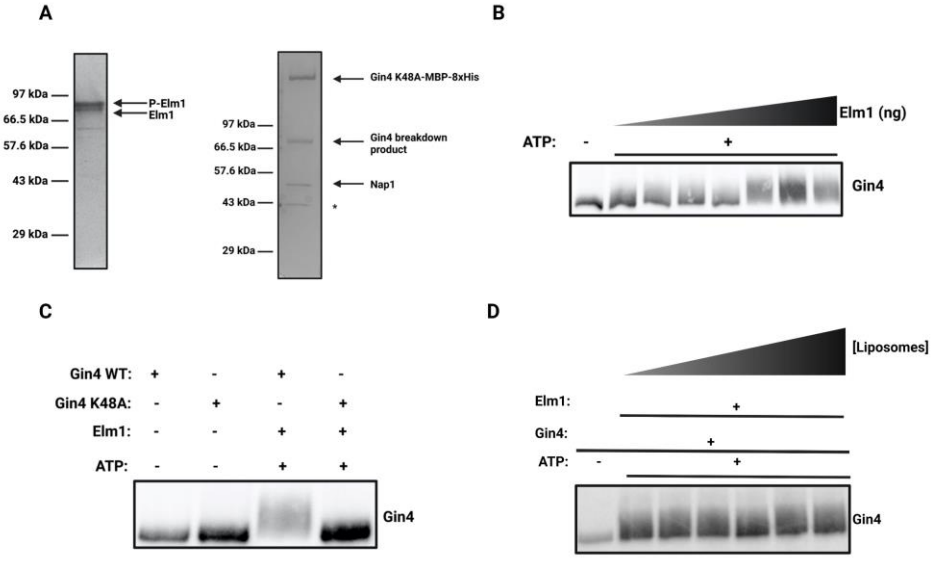

Figure 3. Elm1 directly stimulates Gin4 autophosphorylation *in vitro*. A) Coomassie-stained gel images showing purified Elm1 and kinase dead Gin4 used for *in vitro* kinase assays. B) Purified Gin4 kinase was incubated with ATP on its own, and in other reactions with increasing amounts of purified Elm1 kinase ranging from 20-700 (ng) in the presence of ATP at 30 ◦C for 1 hour. Gin4 phosphorylation was assayed by electrophoretic mobility gel shift via western blotting. This western blot is representative of an experiment with n =3. C) Purified wild type and kinase dead Gin4 kinases were incubated with Elm1 kinase in the presence of ATP at 30 ◦C for 1 hour. Gin4 phosphorylation was assayed by electrophoretic mobility gel shift via western blotting. The first two lanes are control samples of wild type and kinase dead Gin4 kinase in the absence of ATP, respectively. This western blot is representative of an experiment with n =3. D) Purified Gin4 was incubated with purified Elm1 as described in figure 3B. In this experiment increasing amounts of PS-containing liposomes were introduced as represented in this figure. This western blot is representative of an experiment with an n=3.

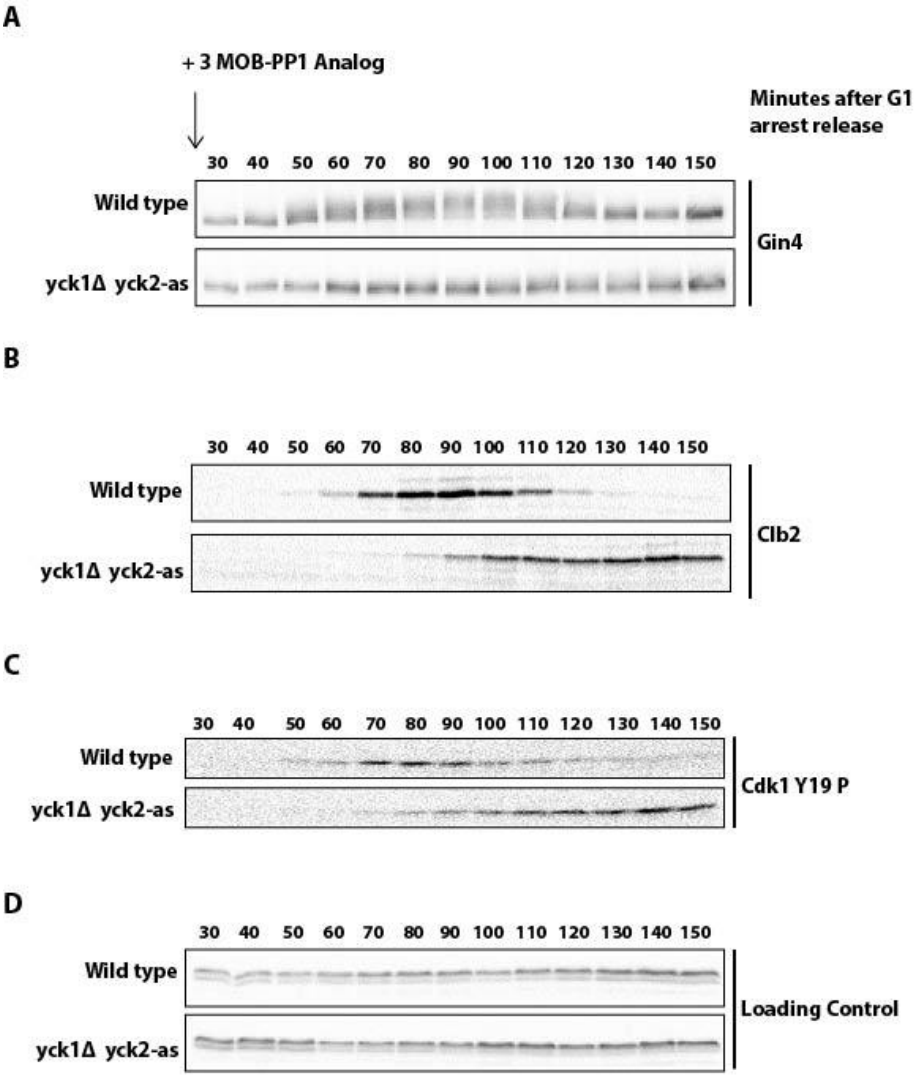

Figure 4. Yck1/2 kinase activity is required for Gin4 hyperphosphorylation and normal mitotic progression *in vivo*. Wild type cells and yck1Δ yck2-as cells were released from a G1 arrest in YPD-ADE growth medium at room temperature and treated with 3-MOB-PP1 analog 15 minutes after release from the G1 arrest. Samples were collected every 10 minutes until the end of the time course and processed for SDS-PAGE. A) Changes in Gin4 phosphorylation, B) Clb2 mitotic cyclin, and C) inhibitory Cdk1 Y19 phosphorylation were tracked via western blotting. D) A loading control was accounted for by probing for Nap1 protein.

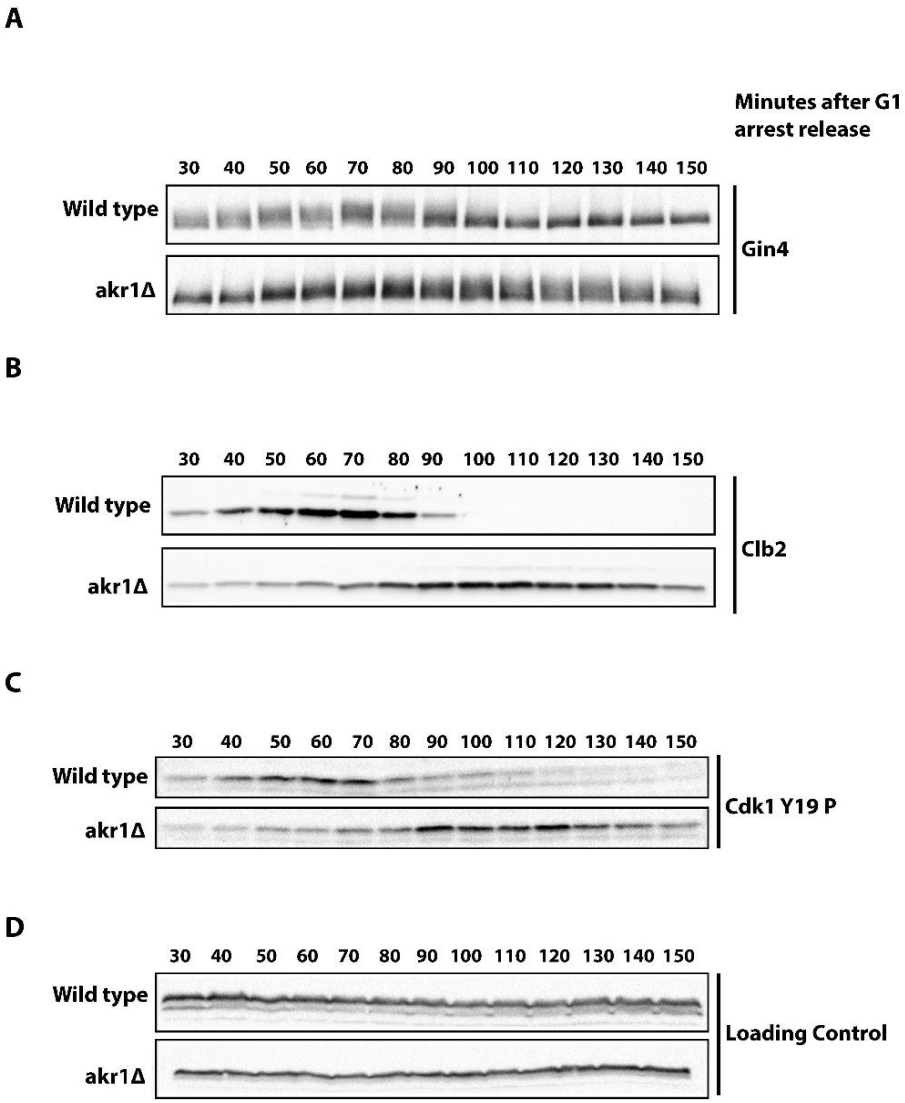

Figure 5. Yck1/2 localization to the plasma membrane is required for Gin4 hyperphosphorylation and normal mitotic progression *in vivo*. Wild type cells and akr1Δ cells were released from a G1 arrest in YPD growth medium at room temperature. Samples were collected every 10 minutes until the end of the time course and processed for SDS-PAGE. A) Changes in Gin4 phosphorylation, B) Clb2 mitotic cyclin, and C) inhibitory Cdk1 Y19 phosphorylation were tracked via western blotting. D) A loading control was accounted for by probing for Nap1 protein, a housekeeping protein in yeast.

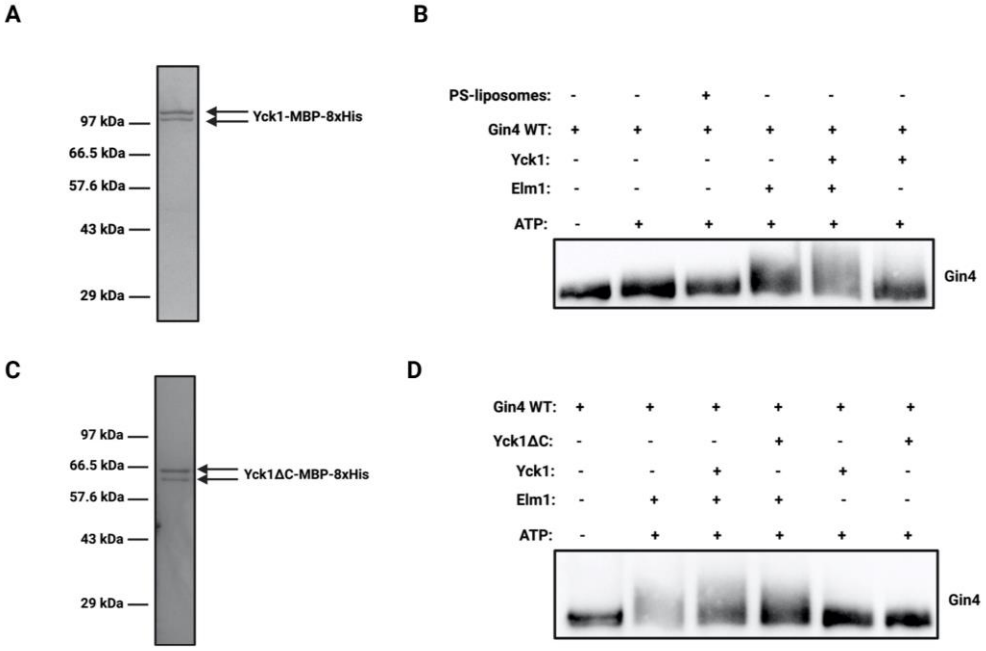

Figure 6. Yck1 stimulates Gin4 autophosphorylation in an Elm1-depedendent manner *in vitro*. A) Coomassie-stained gel image showing purified full-length Yck1 kinase used for *in vitro* kinase assays. B) Purified Gin4 kinase was incubated with ATP on its own, and in varying conditions with purified Yck1, Elm1, and PS-containing liposomes as shown in the figure, in the presence of ATP at 30 C for 1 hour. Gin4 phosphorylation was assayed by electrophoretic mobility gel shift via western blotting. This western blot is representative of an experiment with n =3. C) Coomassie-stained gel image showing purified kinase Yck1Δ kinase used for *in vitro* kinase assays. D) Purified Gin4 kinase was incubated with ATP on its own, and in varying conditions with purified full-length and truncated (ΔC) forms of Yck1 and Elm1, as shown in the figure, in the presence of ATP at 30 C for 1 hour. Gin4 phosphorylation was assayed by electrophoretic mobility gel shift via western blotting. This western blot is representative of an experiment with n =3.

A

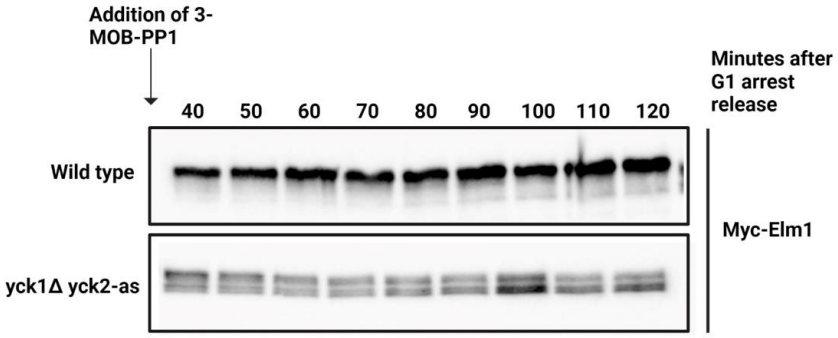

B

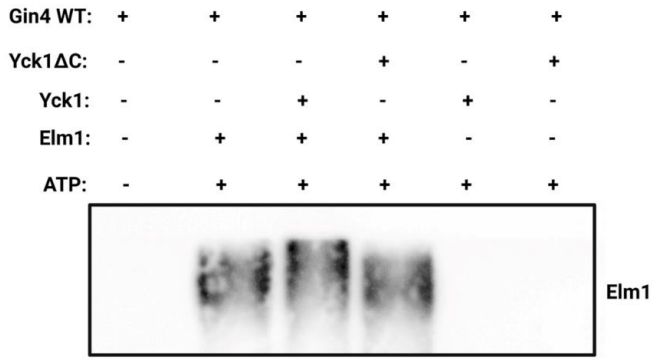

Figure 7. Yck1 promotes hyperphosphorylation and activation of the Elm1 kinase *in vivo* and *in vitro*. A) Wild type cells and yck1Δ yck2-as cells were released from a G1 arrest in YPD-ADE growth medium at room temperature and treated with 3-MOB-PP1 analog 15 minutes after release from the G1 arrest. Samples were collected every 10 minutes until the end of the time course and processed for SDS-PAGE. B) Using the same samples from figure 6D, by western blotting, Elm1 phosphorylation was assayed via electrophoretic mobility gel shift.

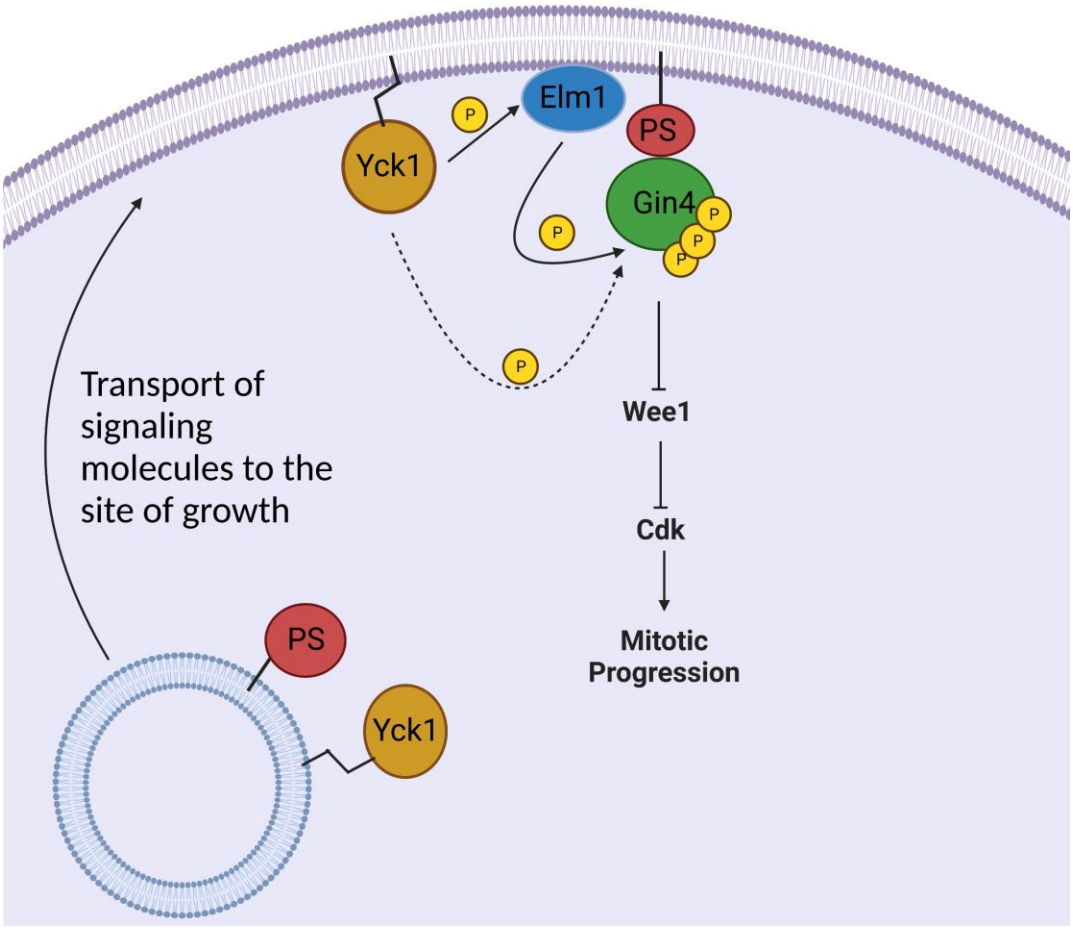

Figure 8. Model for growth-dependent phosphorylation and activation of Gin4 to promote mitotic progression. Shown here is our proposed model in which secretory vesicles deliver phosphatidylserine and Yck1 kinase to the site of growth in response to membrane growth. Phosphatidylserine recruits Gin4 to the plasma membrane where it undergoes autophosphorylation, stimulated by the Elm1 kinase in an Yck1-dependent manner. An alternative mechanism is that Elm1 and Yck1 both act to phosphorylate and drive Gin4 autophosphorylation. Once Gin4 is hyperphosphorylated, it becomes fully active to drive inhibition of Wee1/Swe1, inducing high level activity of Cdk1, leading to metaphase to anaphase transition.

Chapter 3: Identification of Gin4-binding proteins via affinity mass spectrometry

Introduction

Prior to chapter 2 thesis work, information about the proteins Gin4 bind to *in vivo* was limited. Previous Co-immunoprecipitation experiments have identified the septins as the main binding partners of the Gin4 kinase, in its hyperphosphorylated form (Mortensen 2002). However, other binding partners have not been identified in these screens, as Co-IP experiments may not be as sensitive to other affinity binding methods in detecting protein interactions. We sought to conduct a more sensitive binding affinity experiment to identify Gin4 binding partners *in vivo*. To do so, we expressed and purified full-length wild type GST-tagged Gin4 and kinase dead GST-tagged Gin4 proteins from *E. coli* (Figure 1). We developed Gin4 affinity columns by coupling purified wild type and kinase dead Gin4 proteins to Affigel 10 beads, which covalently attaches GST-tagged Gin4 protein to those beads. With this approach, we can make affinity columns with milligram quantities of recombinant protein, allowing an excess of possible Gin4 binding sites for its binding partners, making it a more suitable and sensitive approach to identifying Gin4-binding proteins under different conditions, with the caveat that the Gin4 protein may be linked to the affinity 10 column in different ways that possibly block binding to target proteins. As a control for these large-scale pull-down experiments, we prepared a GST tag affinity column. To reduce background from yeast extracts, we prepared and used a BSA affinity

column. We ran wild type yeast extract in series at a very slow flow rate over a BSA column, followed by a kinase dead Gin4 column, followed by a wild-type Gin4 column, and finally though a GST control column. Columns were washed individually with low salt buffer, and high-binding proteins were eluted by running high salt buffer over the column. We decided to conduct the same experiment using gin4Δ yeast extract to ensure that the proteins that are binding to Gin4 is only biased towards recombinant Gin4 kinase from E. coli and not targeted towards yeast Gin4 kinase. A summary of the Gin4 binding protein affinity experiment is summarized in Figure 2A. By running our elution samples and visualizing protein bands via Coomassie staining, we observed more proteins bound to wild-type Gin4 compared to kinase dead Gin4 (Figure 2B). We concentrated a small portion of our eluted Gin4 binding proteins from GST control, wild type Gin4, and kinase dead Gin4, then sent off for whole-sample mass spectrometry analysis. The mass spectrometry experiment identified over 1,400 potential Gin4 binding partners, which may be either direct or indirect binding partners found in complex with Gin4. In general, we identified potential kinase candidates that may phosphorylate Gin4, phosphatases that may act on Gin4, and proteins involved in ribosome biogenesis. Identification of these Gin4-binding partners *in vivo* could provide mechanistic insight into the factors that regulate Gin4 kinase activity and substrates that Gin4 regulates in mitosis.

Partial Gin4 kinase activity is minimal and sufficient to bind the septins

As a positive control experiment, we decided to first confirm whether septins bind to wild type and kinase dead Gin4 from elution samples extracted from

gin4Δyeast cells to remove any yeast Gin4 background effects. Using specific polyclonal antibodies of Cdc11 and Shs1 septins, binding of these septins occurs with wild type Gin4 and not kinase dead Gin4, as expected (Figure 3). By treating wild type and kinase dead Gin4 eluate samples with lambda protein phosphatase, in4 undergoes partial autophosphorylation in *E. coli*, but kinase dead Gin4 does not undergo autophosphorylation, as expected (Figure 3A). Interestingly, here we show that partial autophosphorylated Gin4 is minimal and sufficient to bind Cdc11 and Shs1, which is a key difference from the Mortensen paper (Mortensen 2002) where it is shown that hyperphosphorylated form of Gin4 binds Cdc11 and Shs1 (Figure 3B). These results suggest that the sites undergoing autophosphorylation *in vitro* by Gin4 expressed in E. coli may be biologically relevant, and therefore, real *in vivo* phosphorylation sites. In addition, it suggests that septin binding may be a biochemical event that occurs before full Gin4 hyperphosphorylation and activation is achieved *in vivo*.

Kinase candidates found in the mass spectrometry experiment

We identified many kinase candidates but based on our cut-off criteria of the mass spectrometry data, which is selecting kinase candidates with a log 2 ratio of quantified protein of wild type Gin4 binding proteins to quantified protein of GST control proteins of 2.5 or higher. With this cutoff criteria, we shortened the list to 24 candidates (Table 1). Two possible models exist with these candidates: Gin4 kinase activity is regulated by these candidates by direct phosphorylation *in vivo*, or Gin4 acts on these kinases to regulate their activity by direct phosphorylation. Surprising

hits included the redundant paralog of Gin4, Hsl1, and Cdc28, which were not previously identified in the HA immunoaffinity pull down experiment (Mortensen 2002). Our data illustrate the better sensitivity of the Gin4 affinity column experiments performed here. Other hits included the Tor1 and Tor2 kinase subunits of TORC1/2 complexes, Ckl1, Fus3, Hrk1, Hrr25, Pkh2, Rio1/2, Rim11, Cdc5, Frk1, Ste7, Akl1, Ptk2, Kin4, Alk1, Kin2/4, and among other hits. Surprisingly, kinases that have been shown to be required for Gin4 hyperphosphorylation *in vivo*, including Elm1 and Cla4 kinases (Mortensen 2002), did not bind to Gin4. However, it is known that many kinases undergo transient interactions with their substrates, so this could be a reason why we can't detect physical interactions with these kinases or other proteins that Gin4 may bind *in vivo*.

We decided to test the genetic requirement of a few of these candidates for Gin4 hyperphosphorylation *in vivo* by deleting or conditionally inactivating kinase candidates. We grew null mutants of Hsl1, Kin3, Kin4, casein kinase Hrr25, Kcc4, Lcb4/5, and Bck1, along with wild type cells and arrested the cells in metaphase using nocodazole, a chemical that disrupts mitotic spindle formation. By arresting cells in metaphase, we can detect a hyperphosphorylated form of Gin4 in wild type cells. We observed no changes in hyperphosphorylation in the absence of these kinase candidates (Figure 4A). Other kinase candidates that we tested included the Tor2 kinase subunit of the TORC2 complex, the polo-like kinase Cdc5, Pkh1/2, and Cbk1. Due to the inability to delete these genes, resulting in cell inviability, we conditionally inactivated kinase activity of these candidate kinases. We inactivated

Tor2 and Cdc5 kinases using temperature-sensitive mutant forms of these kinases. Tor2 and Cdc5 temperature sensitive mutants were grown at room temperature, then shifted to 34 C to activate mutants. We observed a failure of Gin4 hyperphosphorylation in tor2 and cdc5 temperature sensitive mutants compared to wild type mitotic arrested cells (Figure 4B). To determine if Tor2 and Cdc5 act on Gin4 directly, we conducted Gin4 *in vitro* assays using immunopurified HA-tagged Tor2 and Cdc5 kinases on beads. Neither kinase phosphorylated Gin4 *in vitro* (not shown). The genetic dependence of these kinases could be explained by these two kinases regulating another downstream kinase(s) that directly phosphorylate Gin4. For the Tor2 genetic dependency on Gin4 phosphorylation *in vivo*, it is possible that inactivating Tor2 inhibits the TORC2 complex activity, which is known to be a requirement for cell growth (Schmelzle 2000). Furthermore, we know that Gin4 phosphorylation is dependent upon growth (Jasani 2020), therefore, inactivating Tor2 may have reduced cell growth, leading to the failure of full Gin4 hyperphosphorylation under these conditions.

We also tested the genetic dependence of Pkh1/2 kinases in a pkh2Δ pkh1-analog sensitive mutant. To inactivate Pkh1, we treated the mutant cells with adenine analog 1-NM-PP1, which blocks ATP from binding Pkh1, diminishing Pkh1 kinase activity. We observed no changes in Gin4 hyperphosphorylation in a pkh1/2 mutant (Figure 4C). We inactivated Cbk1 also using an analog-sensitive mutation and blocking the ATP binding site with the addition of 1-NM-PP1 drug. We observed no changes in Gin4 hyperphosphorylation in a cbk1-as mutant (Figure 4C). In summary,

Tor2 and cdc5 appear to be kinase candidates that are required for Gin4 hyperphosphorylation *in vivo*, however, not in a direct manner it appears. The other kinase candidates mentioned here appear to be genetically downstream of Gin4, providing insight on possible Gin4 substrates in mitosis. In terms of direct regulators of Gin4 kinase activity *in vitro*, Elm1 and Yck1, which were not identified in the mass spectrometry screen seem to be the key players in driving Gin4 hyperphosphorylation as discussed in chapter 2. However, there are kinase candidates that remain to be tested in the future. Doing so will provide a genetic map on upstream regulators of Gin4 kinase activity and downstream substrates that Gin4 may regulate *in vivo*.

Phosphatase candidates found in the mass spectrometry experiment

The Gin4 kinase undergoes gradual phosphorylation in response to cell growth (Jasani 2020). One mechanism behind the gradual increase in Gin4 phosphorylation is a kinase-driven stepwise phosphorylation as proposed in chapter 2 work. The alternative or complementary model is that a phosphatase or multiple phosphatases act on the kinases that phosphorylate Gin4 or act on Gin4 directly to limit the extent of phosphorylation, resulting in the gradual increase in Gin4 phosphorylation we see *in vivo*. Identifying phosphatases that bind to Gin4 could provide insight on these possible mechanisms of maintaining gradual Gin4 phosphorylation events *in vivo*. From the mass spectrometry data, we identified 11 phosphatase candidates based on our candidate cut-off criteria as mentioned earlier (Table 2). Candidates include Type 2C protein phosphatase Ptc1, ceramide-activated,

type 2A-related phosphatase Sit4, protein tyrosine phosphatase Mih1, PPZ1/2, PP2A subunits, and among other hits. Due to the transient interaction nature between most phosphatases and their substrates, we most likely missed phosphatases that may interact with Gin4 directly or in complex with other factors. Phosphatases not found in our mass spectrometry screen or that did not meet our candidate cut-off criteria include PP2A-Cdc55, PP2A-Rts1, and Cdc14, which were previously tested for genetic dependence on Gin4 phosphorylation *in vivo* in null mutants of the PP2A regulatory subunits Cdc55/Rts1 and Cdc14. If any of these phosphatases are required for gradual increase of Gin4 phosphorylation, we would expect to see accelerated and an increase in the extent of Gin4 phosphorylation *in vivo*.

Deleting Cdc55 and Rts1 PP2A subunits did not result in this phenotype, suggesting that PP2A phosphatase bound to either Cdc55 or Rts1 regulatory subunit do not oppose Gin4 phosphorylation *in vivo*. However, deleting Cdc14 results in prolonged Gin4 hyperphosphorylation and seems to be "stuck" in the hyperphosphorylated state. However, no acceleration of Gin4 phosphorylation was observed nor did the extent of Gin4 phosphorylation increase in the absence of Cdc14. One interpretation of this result is that Cdc14 is required for the dephosphorylation of Gin4 at the end of mitosis. However, the counter argument is that cdc14 null mutant arrest in metaphase (Visintin 1998), explaining why Gin4 remains hyperphosphorylated. To determine if Cdc14 does indeed act on hyperphosphorylated Gin4, an *in vitro* phosphatase assay would need to be carried out.

As for candidates that met our cut-off criteria, we decided to test if Ptc1 phosphatase is required for the gradual increase in Gin4 phosphorylation *in vivo*. Deleting Ptc1 did not result in any Gin4 phosphorylation pattern changes in a synchronized time course experiment (Figure 5A). Even with no changes in Gin4 phosphorylation in the absence of Ptc1, is known that Ptc1 indirectly (genetically) or directly (biochemically) bind Gin4 regulators Cla4, Elm1, and Gin4 itself, all found to be genetically required for Gin4 phosphorylation *in vivo* (Bandyopadhyay 2010, Constanzo 2010 & 2016, Fiedler 2009, Ptacek 2005, Sharifpoor 2012). Another mass spectrometry candidate we tested is Sit4, in which its phosphatase activity is regulated by Sap155/185/190 subunits (Luke 1996). We generated a sap185/190 double deletion yeast strain and asked if Gin4 still undergoes gradual hyperphosphorylation in this mutant strain *in vivo* compared to wild type cells. Inactivation of Sit4 phosphatase by deleting Sap185/190 lead to a delay in Gin4 phosphorylation, but the extent of hyperphosphorylation remained the same (Figure 5B). We attempted to test a sit4 null mutant, but this mutant had difficulties releasing from a G1 arrest, not allowing us to track changes in Gin4 phosphorylation in a cell cycle event. One possible explanation is that sit4 null mutants are hypersensitive to alpha mating factor used to synchronize cells in the G1 phase, making it harder for these cells to escape a G1 arrest. One possible experimental approach to overcome this technical challenge is to introduce a null mutation of sit4 in a strain that contains the BAR gene, which encodes a protein that contributes to breakdown of alpha factor, helping cells escape from a G1 arrest a lot faster than cells that lack the BAR gene.

Based on these results, Sit4 does not seem to be the phosphatase that acts on Gin4 phosphorylation *in vivo*. Remaining candidates are yet to be tested, but doing so will provide insight on how Gin4 hyperphosphorylation is regulated and maintained *in vivo*.

Ribosome Biogenesis Candidates

Ribosome biogenesis is a process that is interconnected with cell growth (Nanduri and Tartakoff 1995, Li 2000, Jorgensen 2004), which is regulated by the TORC1 complex (Mayer and Grummt 2006). Tor1 was a top hit in our kinase candidate list generated from our mass spectrometry data. From the mass spectrometry data, we identified 27 ribosome biogenesis candidates based on our candidate cut-off criteria (Table 3). There are three possible scenarios on why we observed ribosome biogenesis proteins show up in our data. First, ribosome biogenesis is known to consist of housekeeping proteins that may just be considered "background" proteins in our analysis. Second, ribosome biogenesis is a requirement of Gin4 hyperphosphorylation *in vivo*. Interestingly, all our hits bind more efficiently to wild type Gin4 compared to kinase dead Gin4, suggesting Gin4 kinase activity is required for binding events between Gin4 and ribosome biogenesis proteins. Finally, the last possible scenario is that the processes of ribosome biogenesis require Gin4 kinase activity. The fact that we see unique differences in quantified ribosome biogenesis proteins in wild type and kinase dead Gin4 leads us to believe that we are not simply looking at "background" proteins. To distinguish between the last two scenarios on how ribosome biogenesis proteins may relate to Gin4, we will need to

develop genetic tools. Now, studying the link between ribosome biogenesis and the Gin4 kinase is not at high priority. However, once we are ready to address these questions, we will determine if ribosome biogenesis is a requirement of Gin4 hyperphosphorylation *in vivo*, by inactivating key ribosome biogenesis proteins (Ytm1, Ebp2, and Rrp1) involved in maturation of ribosomal RNA and first step of ribosome assembly (Horsey 2004, Miles 2005, Shimoji 2012), and track changes in Gin4 phosphorylation in a synchronized time course experiment. To inactivate these proteins, we will use temperature sensitive yeast strains of these genes, which were obtained from the Woolford lab in Carnegie Mellon University. If Gin4 phosphorylation is decreased or diminished under these mutant conditions, the data would suggest the ribosome biogenesis is required for Gin4 hyperphosphorylation *in vivo*. The data would make sense because ribosome biogenesis contributes to an increase in cell growth by promoting accumulation of mass via the assembly of ribosomes and translation of many proteins. On the other hand, if ribosome biogenesis is not required for Gin4 hyperphosphorylation, the data could suggest Gin4 is upstream of ribosome biogenesis. To test this hypothesis, we will take advantage of a TAP-tagged Nop7 protein that is known to pull down with preribosome assemblies under normal conditions, from early to very late nuclear stages (Miles 2005). We can determine if Gin4 is required for this normal pulldown in a gin4Δ background. If Nop1 is not able to efficiently bind preribosomes, the data could suggest the Gin4 is required for ribosome biogenesis. The alternative experiment would be to study changes in Nop7 pulldown in a kinase dead Gin4

background to determine if kinase activity is required for this process. Regardless, if we see any effects on both major experiments proposed for determining if Gin4 phosphorylation events are upstream or downstream of ribosome biogenesis will link both processes for the first time in our field.

Materials and Methods

Bacterial and yeast strain construction, media, and reagents

All bacterial strains are in the soluble BL21 *E.coli* background and all the yeast strains are in the W303 background (leu2-3, 112 ura3-1, can1-100, ade2-1, his3-11, 15 trp1-1, GAL+, ssd1-d2). Bacterial cells were grown in 2xty media (tryptone, yeast extract, NaCl) with ampicillin supplemented at 100 ug/mL final concentration. Yeast cells were grown in YP medium (yeast extract, peptone, 40 mg/L adenine) supplemented with dextrose (YPD).

To generate bacterial strains, traditional bacterial heat shock transformation protocol was used from NEB. GIN4 expression plasmids were first constructed. Briefly, a full-length wild type GIN4 ORF, tagged with a His6 tag at the C-terminus, fragment along with SalI and NotI restriction sites were PCR-amplified from wild-type yeast genomic DNA. Both the PCR-amplified DNA and a pGEX 4T3 plasmid were digested with SalI and NotI overnight at 37 C. Ligations with T4 DNA ligase were conducted and successful ligations were confirmed by sanger sequencing. The GIN4 plasmid was then transformed into Soluble BL21 *E. coli* cells. Bacterial strains

containing kinase dead GIN4 were constructed in a similar way, except different yeast genomic DNA were used to amplify individual gene fragments.

To generate yeast strains, gene deletion was performed by standard PCR amplification and homologous recombination. Briefly, a sap185Δ sap190Δ strain was developed by the transformation of a PCR-amplified DNA fragment with 40 bp homologous arms of the SAP185/190 genes outside its coding region with KanMx drug selection and HIS nutritional selection markers, respectively. All other strains mentioned in this chapter were previously constructed by the Kellogg Lab and in stock.

Affigel-10 beads were purchased from Bio-rad. Reagents for mass spectrometry were a gift from Steven Gygi. Polyclonal antibodies were homemade. All other reagents were bought from sigma-aldrich.

Purification of GST-Gin4 protein fusions and Lambda Phosphatase treatment

Purification of GST-Gin4 fusion proteins from bacteria was carried out using traditional affinity chromatography methods. Briefly, liters worth of transformed-bacteria for all Gin4 fusions (wild-type and kinase dead) were grown in 2xty medium plus ampicillin (100 μg /mL) at 37 ˚C until OD600 was 0.8.-1.0. Cells were then shifted to room temperature prior to induction. Expression for GST-Gin4 fusions were induced by the addition of IPTG at a final concentration of 0.2 mM at room temperature for 3 hours. Cells were pelleted at 4 ˚C and supernatant was discarded. Cell pellets were frozen in liquid nitrogen, then grounded in a coffee grinder with dry

ice to avoid overheating. Cell powder was stored at 80 ˚C overnight to allow dry ice CO2 to evaporate. To create bacterial extracts, 16 g of powder per strain were resuspended in 4 volumes of lysis buffer (50 mM HEPES-KOH pH 7.6, 1 M KCl, 0.5% Tween-20, and 2 mM PMSF). Cell suspensions were pelleted at 4 ˚C for 1 hour at 40,000 rpm, then the supernatant was kept. Crude extracts were loaded onto a 5 mL glutathione-agarose column, pre-equilibrated with lysis buffer without PMSF, at a 45 mL/hr flow rate using a pump system at 4 ˚C. The column was then washed with 15 column volumes of washing buffer (lysis buffer without PMSF) at a flow rate of 60 mL/hour at 4 C. The column was then transferred to room temperature and washed with 2 column volumes of elution buffer without reduced glutathione. GST-Gin4 fusions were eluted off the column in 1.5 mL fractions using elution buffer (50 mM HEPES-KOH pH 7.6, 150 mM KCl, 2 mM MgCl2, 10 mM reduced glutathione, and 10% glycerol). Elution of the GST-Gin4 fusions were monitored by conducting a Bradford assay for each fraction. Peak elution fractions were pooled and dialyzed against a 50 mM HEPES pH 7.6, 150 mM KCl, and 30% glycerol buffer. The result is a GST-Gin4 fusion with breakdown products specific to Gin4, due to proteolysis. Per GST-Gin4 protein (wild type and kinase dead), a yield ranging from 5-8 mg total was achieved and used for coupling to affigel 10 beads for Gin4 affinity experiments. A small sample of wild type and kinase dead Gin4 proteins were treated with Lambda Phosphatase in the presence of 1 mM MnCl2 to confirm Gin4 kinase activities of both proteins.

Purification of Gin4-binding proteins from yeast cells and preparation of protein samples for mass spectrometry

To purify Gin4-binding proteins, wild-type and gin4Δ yeast extracts were separately loaded onto Gin4 affinity columns. Briefly, 5-8 mg of either GST-Gin4 WT or GST-Gin4 kinase dead were coupled to 1.5 mL of affigel 10 beads using a Kellogg Lab ready protocol. To create yeast extract, liters worth of wild-type yeast cells were grown in YPD medium overnight at 30 ˚C until cells reached OD_{600} of 0.6-0.8. Cells were pelleted at 4 ˚C for 10 minutes at 5,000 rpm and the supernatant was removed. Cell pellets were frozen in liquid nitrogen, transferred to a coffee grinder with dry ice and grounded to make a powder. The powder was then stored at -80 ˚C overnight to allow the dry ice CO2 to evaporate. Next, yeast cells were further grounded in liquid nitrogen using a mortar and pestle to achieve lysis. 9 g of cells were resuspended in 25 mL of extract buffer (50 mM HEPES-KOH pH 7.6, 150 mM KCl, 1 mM MgCl2, 1 mM EGTA, 0.15% Tween-20, 1 mM DTT, 2 mM PMSF, and 10% Glycerol).

Yeast crude extract was then loaded onto a 5 mL BSA affigel column, which was used as a filter to remove non-specific proteins found in the lysate. Followed by the BSA column, the lysate was run over a kinase dead GST-Gin4 affigel column, followed by a wild-type GST-Gin4 affigel column, and finally over a GST only affigel column, used as our control for these affinity chromatography experiments. All columns, except for BSA, were washed separately by gravity flow using 10 column volumes of washing buffer (like extract buffer, except Tween-20

concentration is 0.05%). Finally, Gin4-binding proteins were eluted off the columns in 200 µLfractions using a high salt elution buffer (50 mM HEPES-KOH pH 7.6, 1 M KCl, 1 mM MgCl2, 0.05% Tween-20, 1 mM DTT, and 10% glycerol). Elution of the Gin4-binding proteins were monitored by conducting a Bradford assay for each fraction. Peak fractions were pooled together.

To prepare samples for mass spectrometry, $1/15^{th}$ of total pooled peak elution sample from the GST control and $1/10^{th}$ of total pooled peak elution sample from wild-type Gin4 were TCA precipitated. Briefly, elution samples were treated with $1/10^{th}$ of TCA and incubated on ice for 5 minutes. Samples were then pelleted at room temperature for 5 minutes at 14,000 rpm. The supernatant was removed, and a second spin was conducted to remove excess liquid. Protein pellets were then washed with 200 µL of acetone and spun for 5 minutes at 14,000 rpm. Acetone was then removed, and protein pellets were air-dried. Please note that for the first set of mass spectrometry samples, I did not process samples for kinase dead Gin4. The second set of samples were processed like the first set, except this time we used elution samples from gin4Δ extract and this time we processed a sample from the kinase dead Gin4 elution. Samples for mass spectrometry were sent to the Steven Gygi laboratory and further processed there for tandem-mass tag MS. Please check tables in this chapter to learn about our candidate selection criteria.

Probing for Septin-Gin4 interactions via western blotting

Leftover elution samples from the wild type Gin4 and kinase dead Gin4 columns not prepared and processed from mass spectrometry analysis were used to probe for Gin4 interactions with Cdc11 and Shs1, two out of the 5 septins in yeast via western blotting. A portion of the elution samples were mixed with 14 µL of 1x sample buffer (65 mM Tris-HCl pH 6.8, 3% SDS, 10% glycerol, 5% beta-mercapethanol, and bromophenol blue), then boiled for 5 minutes, followed by a quick centrifugation step using a table-top microcentrifuge. 2 µL of each sample were loaded into a 9% polyacrylamide gel and proteins were separated by running 20 mA of current. Rapid protein transfer into nitrocellulose using a Biorad semidry turbo blotter was then performed at the normal transfer settings. The nitrocellulose membrane was then blocked in 5% milk solution in 1x PBST (1x PBS, 250 mM NaCl, and 0.1% Tween-20). Blots were probed with primary antibody at 1-2 µg/mL overnight at 4 C in 5% milk PBST solution. Primary antibodies used were anti-Cdc11(1:2000 dilution) and anti-Shs1 (1:3333 dilution). Primary antibodies were detected by using an HRP-conjugated donkey anti-rabbit secondary antibody incubated in 5% milk PBST solution for 1 hour at room temperature. Blots were rinsed in 1x PBST, followed by a final wash in 1x PBS before detection of Cdc11 and Shs1 proteins via chemiluminescence using ECL reagents with a Bio-Rad ChemiDoc imaging system.

Testing of kinase candidates' requirement for Gin4 hyperphosphorylation *in vivo*

To determine if Hsl1, Kin4, Akl1, Kcc4, lcb4/5 and Bck1 are required for Gin4 hyperphosphorylation *in vivo,* we relied on null mutant strains of each kinase candidate. To determine if Tor2 and Cdc5 are required for Gin4 hyperphosphorylation *in vivo,* we relied on the use of temperature sensitive mutant strains of these kinase candidates. Finally, to test if Pkh1/2 and Cbk1 are required for Gin4 hyperphosphorylation on vivo, we inhibited kinase activity by using 1-NM-PP1 as an analog inhibitor of a pkh1 and cbk1 analog sensitive mutation. For null mutant candidate strains, yeast cultures were grown to log-phase overnight at room temperature and arrested in mitosis by adding nocodazole to 10 µg/mL final concentration. Cultures were incubated for an additional 3 hours at room temperature. After 3 hours, 1.6 mL of cells were collected, normalized to OD_{600} of 0.4, and processed for western blotting. Briefly, cells were pelleted, and supernatant was removed. Acid-washed beads were added to cell pellets, frozen in liquid nitrogen, and 140 µL of 1x sample buffer were added to each sample. Samples were bead-beat for 2 minutes, centrifuged for 15 seconds using tabletop microcentrifuge at full speed, boiled for 5 minutes, and centrifuged again for 5 minutes. 10 µL of samples were loaded into 9% polyacrylamide gel and proteins were separated as described above. To probe for Gin4, a Gin4-specific polyclonal antibody was used at a 1:2000 dilution in 5% milk 1x PBST solution. Temperature-sensitive and analog-sensitive kinase candidate samples were processed similarly, however, Tor2 and Cdc5 temperature

sensitive yeast cells were switched to 34 ˚C when treated with nocodazole. pkh1-as pkh2Δ and cbk1-as cells were treated with 1 NM-PP1 analog inhibitor to a 5 μM final concentration after treatment with nocodazole.

Testing of phosphatase candidates' requirement for Gin4 hyperphosphorylation *in vivo*

To determine if Ptc1 and Sit4 are required for Gin4 hyperphosphorylation *in vivo,* we relied on ptc1 null mutant and sap185/90 double null mutant strains. SAP185 and SAP190 are regulatory subunits of Sit4. Cell cycle time course experiments with these were conducted as previously described (Harvey et al. 2011). Briefly, null mutant and wild type cells were grown in YPD medium (yeast extract, peptone, and dextrose) at room temperature for 12-16 hours until cells reached an optical density (OD_{600}) between 0.4-0.7. Cells were synchronized at G1 phase by treating cells for 3 hours at room temperature with alpha mating factor to a final concentration of 0.5 μg/mL. Cells were released from a G1 arrest by three rounds of pelleting followed by resuspension with an equal volume of YPD medium. After the final wash, cells were transferred to 25 ˚C. Starting at 10-20 minutes, depending on experiment, after release from G1 arrest, 1.6 mL samples were collected every 10 minutes until a total of 100 minutes were reached. To ensure one cell cycle event was tracked, alpha factor was added at the same volume, again, at 60 minutes after G1 arrest release. Samples were processed for SDS-PAGE gel electrophoresis and western blotting by: Pelleted cells followed by removal of supernatant. Acid-washed microbeads were added to the pellet and flash-freeze in liquid nitrogen. Cells were lysed by adding 140 μL of 1x

sample buffer (65 mM Tris-HCl pH 6.8, 3% SDS, 10% glycerol, 5% beta-mercapethanol, and bromophenol blue) supplemented with 2 mM PMSF and placed in a mini-beadbeater 16 (BioSpec) at top speed for 2 minutes at 4 ˚C. After, samples were centrifuged followed by boiling at 95 ˚C for 5 minutes, then, centrifuged again for 5 minutes at 15,000 rpm using a table-top microcentrifuge. Protein samples (10 µL) were separated by passing 20 mA of current through a 10% polyacrylamide gel submerged in running buffer (Glycine, Tris base, 10% SDS), then transferred to a nitrocellulose membrane at 4 ˚C using a wet transfer apparatus at 800 mA in 1x transfer buffer (Tris base, glycine, and methanol) when probing for Gin4. Blots were probed with primary antibody at 1-2 µg/mL overnight at 4 ˚C in 5% milk in PBST (1x phosphate-buffered saline, 250 mM NaCl, and 0.1% Tween-20) containing 5% nonfat dry milk. Primary antibodies were detected by using an HRP-conjugated donkey anti-rabbit secondary antibody incubated in 5% milk PBST solution for 1 hour at room temperature. Blots were rinsed in 1x PBST, followed by a final wash in 1x PBS before detection via chemiluminescence using ECL reagents with a Bio-rad ChemiDoc imaging system.

Figures

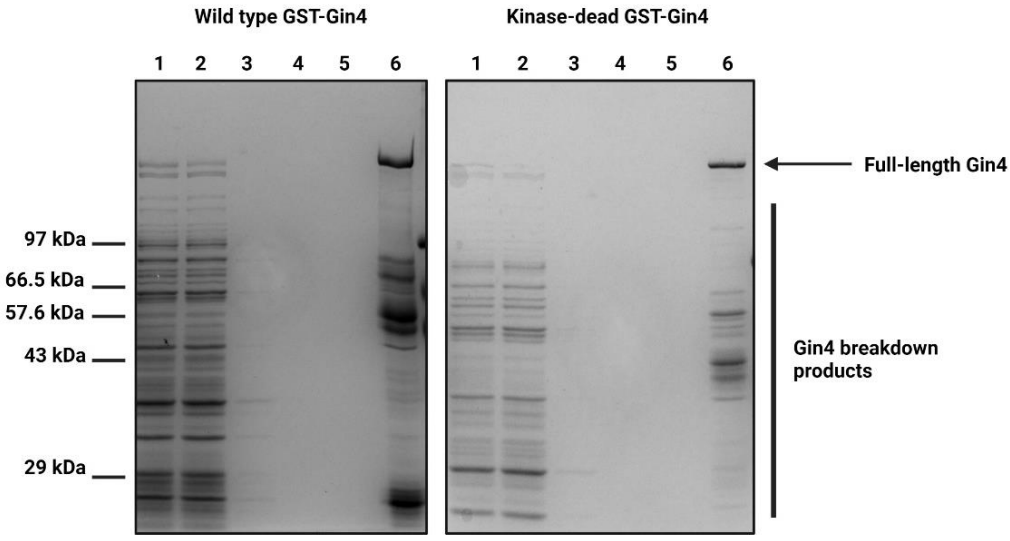

Figure 1. Purification of recombinant wild type and kinase dead GST-tagged Gin4 kinases from *E. coli*. Both wild type and kinase dead Gin4 kinases were expressed and purified from *E. coli* via a single glutathione-agarose column chromatography step. The following is the key to the gel lanes: 1) Cell Extract, 2) Flow-through from column, 3) First Wash, 4) Second Wash, 5) Final Wash, 6) Gin4 Eluate. Full-length Gin4 proteins are labeled by an arrow and breakdown products of Gin4 are labeled below full-length protein.

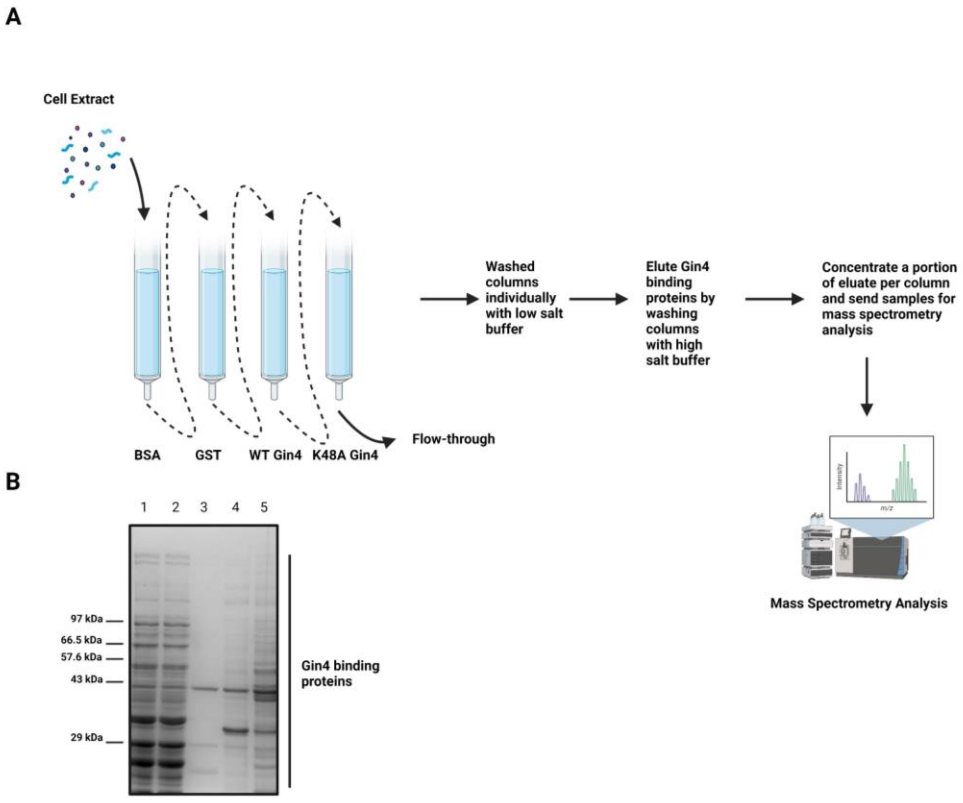

Figure 2. Purification of Gin4-binding proteins via sequential Gin4 affinity chromatography. A) Purification of Gin4 binding proteins workflow, B) Coomassie stained gel showing purified Gin4-binding proteins from different affinity columns. The following is the key to the lanes of the gel: 1) Cell Extract, 2) Flow through from sequential loading, 3) GST control eluate, 4) Kinase dead (K48A) Gin4 eluate, 5) Wild type Gin4 eluate. Gin4-binding proteins are labeled by a vertical black lane.

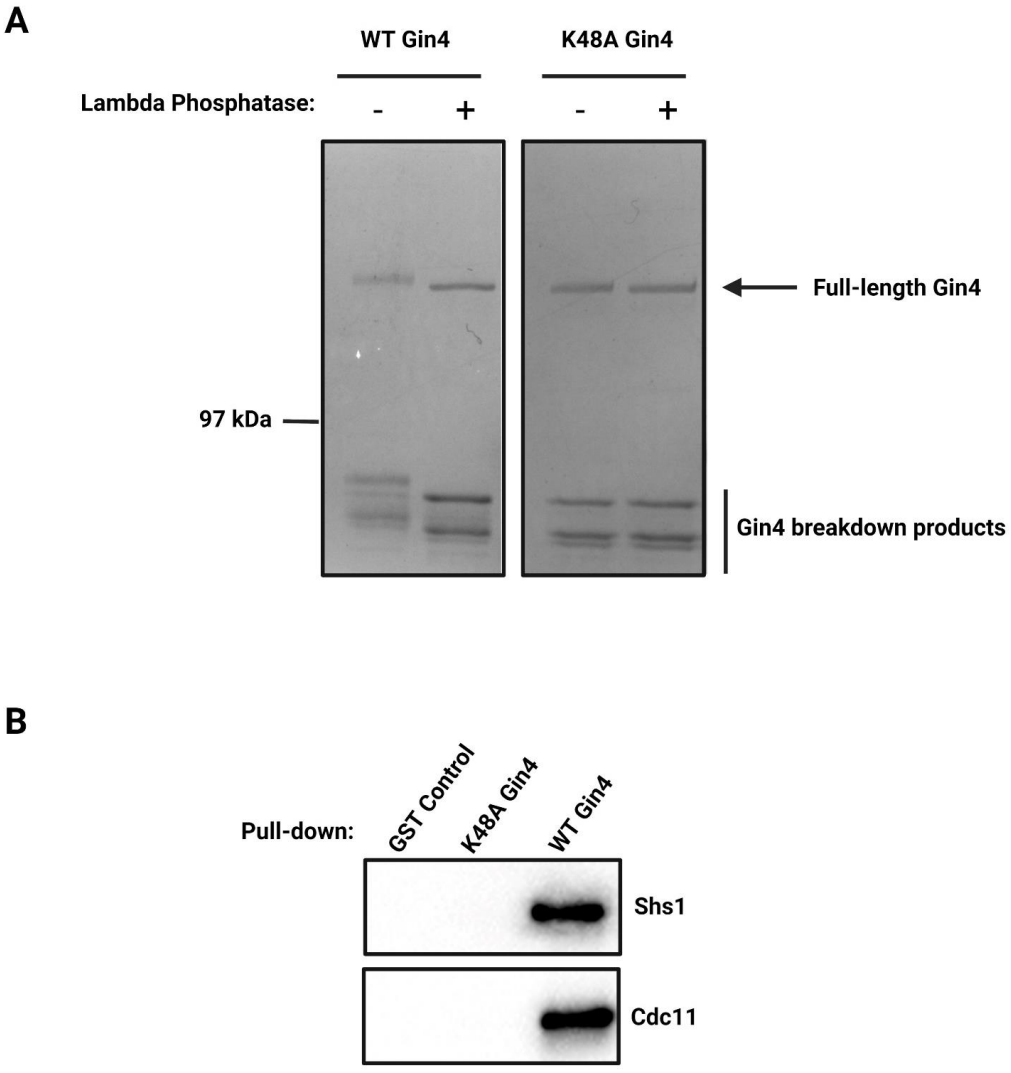

Figure 3. Septin-Gin4 interactions are dependent on Gin4 kinase activity. A) Wild type and kinase dead Gin4 kinases purified from *E. coli* were treated with lambda protein phosphatase in the presence of 1 mM MnCl2. Wild type Gin4 undergoes dephosphorylation upon phosphatase treatment compared to kinase dead Gin4. Full-length proteins are labeled by black arrow and Gin4 breakdown products are labeled by a vertical black line. B) Eluate samples from the sequential Gin4 affinity chromatography experiment were probed for Shs1 and Cdc11 protein. Shs1 and Cdc11 were only present in wild type Gin4 eluate pulldown sample, and not in the kinase dead Gin4 and GST control eluates.

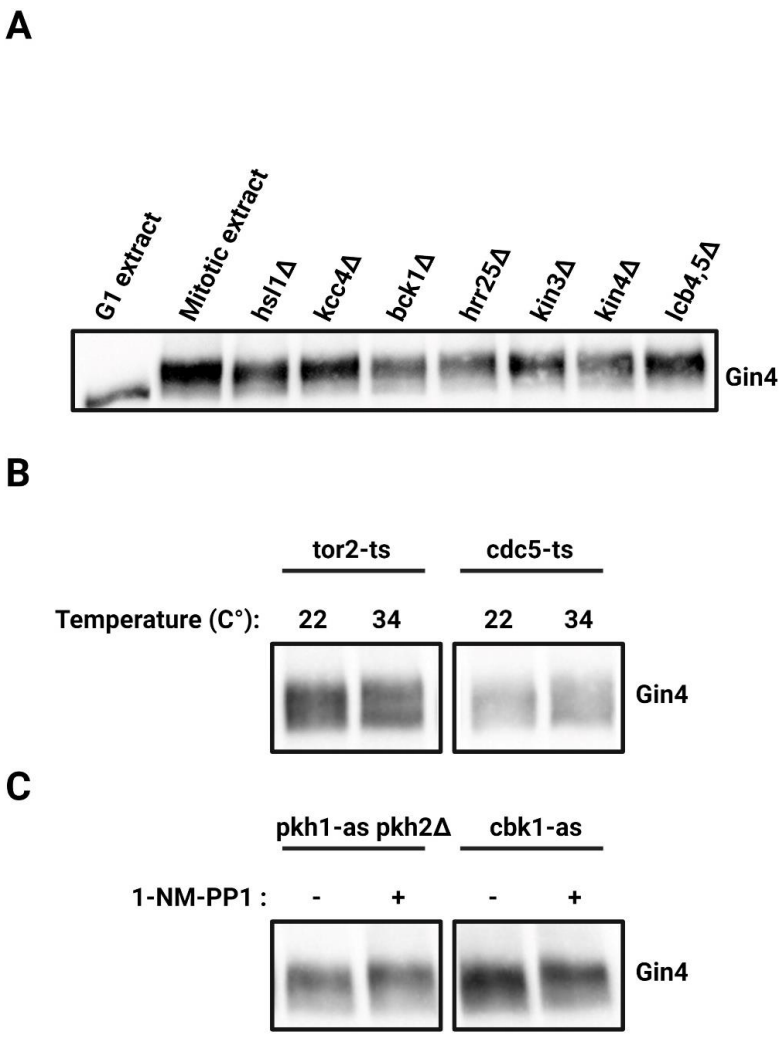

Figure 4. Testing kinase candidates from the mass spectrometry analysis for the genetic requirement of Gin4 hyperphosphorylation *in vivo*. A) Null mutant strains were grown in YPD growth medium to log-phase at room temperature. Samples were processed for SDS-PAGE and probed for Gin4 via western blotting. G1 and mitotic cell extracts were loaded as reference for Gin4 phosphorylation *in vivo*. B) Tor2 and Cdc5 temperature sensitive mutant strains were grown in YPD growth medium, then were shifted to 34 ˚C. Samples were processed for SDS-PAGE and probed for Gin4 via western blotting. C) pkh1-as pkh2Δ and cbk1-as mutant strains were grown in growth medium without adenine to log-phase at room temperature. Cells were split into two flasks; one set of cells were treated with 1-NM-PP1 analog, and the other set of cells were left untreated. Samples were processed for SDS-PAGE and probed for Gin4 via western blotting. In all experiments, cells were arrested with treatment of nocodazole.

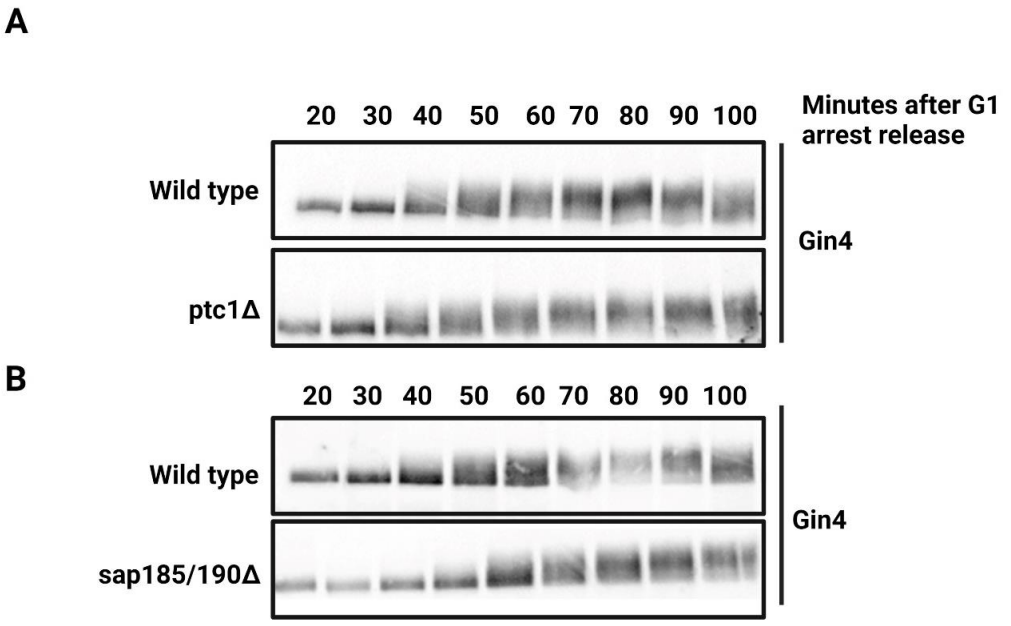

Figure 5. Testing phosphatase candidates from the mass spectrometry analysis for the genetic requirement of Gin4 hyperphosphorylation *in vivo*. A,B) Wild type and null mutant strains were grown in YPD growth medium to log-phase at room temperature. Cells were synchronized in G1 and released from a G1 arrest. Samples were collected throughout cell cycle event, processed for SDS-PAGE, and probed for Gin4 via western blotting.

Tables

Gene Symbol	Number of peptides	Protein Quantification (TMT Signal)			Log2 (WT Gin4/GST control)
		GST control	WT Gin4	Kinase dead Gin4	
GIN4	247	0.938449	64.9766	11.0206	6.1134981
CKI1	45	1.17727	36.525	42.9376	4.955367136
HSL1	101	1.26162	32.5635	29.3291	4.689906431
FUS3	20	2.43133	61.6456	15.7828	4.664180299
CDC28	39	1.86277	43.4063	13.4137	4.542382993
HRK1	5	2.04666	40.6384	18.7411	4.311500241
HRR25	25	2.18487	42.2937	12.571	4.274823431
PKH2	2	1.62136	30.7557	22.2868	4.245577451
RIO2	9	2.08195	36.8545	13.5609	4.145833459
RIM11	4	2.08378	35.7024	30.6709	4.098746184
CDC5	5	2.36767	38.5365	18.825	4.024685627
FRK1	1	1.77413	28.8439	26.9045	4.023082613
AKL1	2	2.18407	33.297	19.8838	3.930301198
KIN4	21	2.28079	30.0584	26.219	3.720162693
TOR2	27	2.3581	30.9587	31.0286	3.714648087
ALK1	13	2.09451	26.9363	29.5467	3.684867017
PRS1	24	5.38822	58.082	11.9023	3.43021047
STT4	56	2.12882	22.5995	23.7452	3.40816498
KIN2	2	3.97722	40.1756	21.1044	3.336487298
CBK1	8	2.9976	28.6991	19.3257	3.259125707
TOR1	3	2.96485	28.2398	30.419	3.251698849
GCN2	1	3.58903	33.5428	30.6091	3.224337236
SGV1	1	4.02974	36.0761	17.0066	3.162284721
LCB5	7	2.46539	21.435	19.1412	3.120080627
KCC4	132	2.6599	22.1344	15.5803	3.056846353
RIO1	6	3.33634	27.5266	15.1723	3.0444882
DBF20	3	7.28604	45.7382	12.1048	2.65019277
KIN3	14	6.91218	37.9444	12.4895	2.45667429
BCK1	2	7.62035	35.9965	18.4363	2.239927471

		Protein Quantification (TMT Signal)			
Gene Symbol	**Number of peptides**	**GST control**	**WT Gin4**	**Kinase-dead Gin4**	**Log2 (WT Gin4/GST control)**
PTC1	32	0.824492	56.3794	10.5266	6.095518819
SIT4	26	1.25011	39.9849	11.037	4.999328328
TPD3	2	0.14239	3.94318	16.1072	4.791439834
PPZ2	21	2.0598	33.9374	27.3217	4.042299874
MIH1	5	2.46398	37.7093	36.7303	3.935857919
CMP2	2	2.00392	29.3584	15.9243	3.872876525
GLC7	8	2.86958	40.7912	25.4655	3.829346449
PPZ1	21	3.14014	36.8198	25.0302	3.551581003
PSR1	1	2.89003	31.7579	13.3115	3.457959143
PPQ1	1	3.49318	36.715	17.6149	3.39375671
PTC4	9	8.41751	48.1281	13.9137	2.515414035

		Protein Quantification (TMT Signal)			
Gene Symbol	**Number of peptides**	**GST control**	**WT Gin4**	**Kinase dead Gin4**	**Log2 (WT Gin4/GST control)**
NIP7	37	1.16019	48.6641	17.4165	5.390424879
BRX1	36	1.27483	50.3338	16.6054	5.30315074
ENP2	37	1.28317	41.8209	14.3269	5.026439887
MAK21	55	1.64303	48.9112	17.2605	4.895734133
TSR1	61	1.04797	28.409	7.52434	4.760678727
SSF2	10	1.58271	41.7745	16.7772	4.722153721
RPF2	45	1.57469	39.4429	20.0146	4.646625882
RLP24	10	1.58924	38.024	16.1847	4.580501391
SLX9	9	1.9322	41.5981	13.9964	4.428201296
SSF1	25	2.14094	45.7021	14.8686	4.415944189
NSA1	27	2.1689	46.055	14.8584	4.40832235
RLP7	27	2.18481	44.1658	15.4791	4.337349916
RRP5	173	2.18836	43.2556	18.0795	4.304964925
UTP30	6	2.47141	48.4983	12.3789	4.294527903
ERB1	55	2.32011	44.4056	14.9899	4.258476514
BMS1	56	2.10483	38.7895	14.1763	4.203890558
YTM1	27	2.52216	45.4581	14.7499	4.171805681
NOP8	20	2.66651	47.342	18.2734	4.150096012
RRP36	5	3.00562	50.7872	22.2647	4.078730411
NOP15	11	2.70769	44.6623	14.4397	4.043923067
NSA2	30	2.22805	33.1685	16.7536	3.895960256
NOP53	25	1.96007	28.8888	19.3832	3.881533194
REH1	15	3.2488	26.1838	14.225	3.01069565
RIX7	5	3.91319	30.0883	21.3311	2.942785531
REI1	16	3.8024	27.588	12.1494	2.85905866
ALB1	18	4.12489	26.5065	13.2326	2.683918633
PEX8	3	7.03142	41.7563	16.0847	2.570105904

Table Legends

For tables 1-3, the names of protein hits are placed under the "Gene Symbol" column. Also shown is the number of peptides identified from the mass spectrometry per protein. Protein quantification is shown as the "TMT Signal" from proteins eluted from GST, wild type Gin4, and kinase dead Gin4 affinity columns. A calculated log2 (WT/GST control) from the TMT signal is shown as well to determine how much protein binds to wild type Gin4 compared to the GST control. Top-hit candidates were selected as those protein hits having a log2 (WT/GST control) of 2.5 or higher.

Table 1 (Page 70). List of kinase candidates from Gin4 affinity mass spectrometry experiment.

Table 2 (Page 71). List of phosphatase candidates from Gin4 affinity mass spectrometry experiment.

Table 3 (Page 72). List of ribosome biogenesis candidates from Gin4 affinity mass spectrometry experiment.

Chapter 4: Effects of Gin4 C-terminal truncations on cell size and mitotic progression

Introduction

The Gin4 kinase undergoes activation via hyperphosphorylation in response to cell growth (Altman 1997). Part of the MARK/PARK kinase activation model predicts that Gin4 kinase may also undergo confirmational changes in its protein structure as it undergoes hyperphosphorylation (Emptage 2018). That is, in its dephosphorylated state, the Gin4 kinase is in its closed confirmation via interactions between the N-terminal kinase and C-terminal KA1 anionic phospholipid domains, to an open confirmation, resulting in a hyperphosphorylated, active Gin4 kinase (Nesic 2010, Emptage 2017). That is assuming that activation of Gin4 and MARK/PARK kinases are conserved mechanisms between budding yeast and mammalian cells. We predict that if reversal of Gin4 autoinhibition in response to growth is the mechanism of activating Gin4, then truncating and removing the KA1 domain should prevent interactions between the Gin4 kinase and KA1 domains, promoting a constitutively active form of Gin4.

Results

Construction of Gin4 C-terminal truncation yeast strains and cell size analysis

To determine a minimally active form of Gin4 in yeast is sufficient to drive normal cell cycle progression, we created strains in which we introduce sequential C-terminal truncations of Gin4 under the control of the GAL1 promoter. We

overexpressed a KA1 domain-deleted Gin4, a linker + KA1 domain-deleted Gin4, and a construct expressing the Gin4 kinase domain (amino acids 1-360), all in individual yeast strains (Figure 1). We decided to overexpress Gin4 because deleting the KA1 domain will disrupt its localization to the bud neck. By overexpressing our Gin4 constructs, Gin4 could overcome any signaling issues that arise from its mislocalization. All Gin4 constructs were tagged with a 3xHA epitope tag for protein visualization and confirmation of truncation via western blotting (not shown).

It is known that Swe1 kinase is activated via direct phosphorylation by Cdk1 shortly after mitotic entry, resulting in a negative feedback loop where Cdk1 is directly phosphorylated and inhibited by active Swe1 at tyrosine 19 in yeast cells (Gould and Nurse 1989, Harvey 2005 and 2011). Cells cannot progress from metaphase to anaphase until the inhibitory of Cdk1 is removed and relieved by the Cdc25 phosphatase (Russell and Nurse 1986, Dunphy and Kumagai 1991, Gautier 1991). Simultaneously, the Swe1 kinase must be hyperphosphorylated and degraded for mitotic progression to occur normally (Mueller 1995). Our current model for Swe1 inhibition prior to the metaphase-anaphase transition in mitosis is that Gin4 inhibits Swe1, as previously shown to be required, genetically, for hyperphosphorylation of Swe1 *in vivo* (Jasani 2020). However, we do not know if this is a direct effect on Swe1. To study if Swe1 is likely a direct target of Gin4 *in vivo*, we decided to carry out a cell size analysis of Gin4 C-terminal truncation yeast strains compared to full-length wild type Gin4 under control of the galactose promoter (GAL1).

The hypothesis is that if Gin4 undergoes autoinhibition via kinase domain and KA1 domain interactions, then truncating the C-terminal region should relieve autoinhibition and result in accelerated Swe1 hyperphosphorylation and inhibition. That is, the more truncated Gin4 gets, cells should divide at a smaller size compared to wild type cells in the presence of galactose. We grew cells to log phase, then measured cell size using a Z2 coulter counter calibrated specifically for yeast cells. Note that we did not do cell size comparisons with overexpressed full-length Gin4, because a Gal-Gin4 strain in the presence of galactose results in an elongated bud phenotype, a dominant-negative genetic effect. Based on the cell size analysis, Gin4 C-terminal truncation cells were smaller in size compared to wild type cells that express full-length Gin4 at endogenous levels (Figure 2). In addition, overexpressing truncated forms of Gin4 did not result in elongated bud phenotypes (not shown), which suggests that overexpressing truncated forms of Gin4 rescue the dominant-negative effect we observe when we overexpress full length Gin4. Interestingly, a Gin4 strain that lacks the KA1 domain has been shown to result in an elongated bud phenotype when expressed under dextrose conditions (Jasani 2020), but here we show overexpressing this strain in galactose rescues this phenotype due to decreased cell size compared to wild type cells. This data supports the hypothesis that Gin4 undergoes autoinhibition and by truncating Gin4, C-terminally, cells accelerate division at a smaller size most likely due to constitutively active Gin4 present, even though it is not localized properly to the bud neck.

Effects of C-terminally truncating Gin4 on mitotic progression *in vivo*

Due to the decreased size effects, we observed in C-terminal truncated Gin4 yeast cells, we hypothesized that mitotic progression is accelerated and, therefore, Swe1 hyperphosphorylation is also accelerated in these cells. To observe effects on mitotic progression and Swe1 hyperphosphorylation, we carried out synchronized cell cycle experiments in all strains except in a Gin4 strain lacking the KA1 domain. However, based on previous work, we know that Gin4 ΔKA1 cells grown in dextrose result in a slight mitotic delay (Jasani 2020), suggesting Swe1 hyperphosphorylation is also delayed or maybe fails to occur.

To track changes in mitotic progression, we used the mitotic cyclin Clb2 as a marker for tracking mitotic timing. Compared to wild type cells, overexpressing the truncated forms of Gin4 resulted in a mitotic delay (Figure 3A), which was surprising to us since we thought smaller cells would imply accelerated cell cycle progression and timing. To track phosphorylation changes in Swe1, we used a Swe1-specific antibody and looked for changes in electrophoretic mobility gel shifts of Swe1. Compared to wild type cells, cells lacking Gin4 Δ500-1143 cells failed to undergo normal Swe1 hyperphosphorylation, yet a mitotic delay was obvious. This data suggests that part of that interdomain flexible linker of Gin4 is inducing a dominant negative effect when overexpressed. In cells overexpressing the Gin4 kinase domain only resulted in no changes to Swe1 hyperphosphorylation *in vivo*, but the point at

which Swe1 undergoes hyperphosphorylation occurs and degrades was delayed, consistent with delayed Clb2 levels (Figure 3B). One possible explanation on why overexpressing C-terminal truncated Gin4 constructs are smaller compared to wild type, yet, have mitotic progression delays could be due to changes in cell growth and growth rate.

Growth rate analysis of C-terminal truncations of Gin4

To determine if truncating the C-terminus of Gin4 sequentially results in growth defects, more specifically, changes in growth rate, we performed a synchronized cell cycle time course experiment. For this study, we only compared changes in growth rate between cells lacking the flexible linker and KA1 domain of Gin4, cells containing only the Gin4 kinase, and wild type cells grown in galactose media. Both C-terminal truncations of Gin4 grew at a slower rate compared to wild type cells (Figure 4). This observation suggests that these cells are smaller because of a reduced growth rate compared to wild type cells. One possible explanation is that by truncating the C-terminal regions of Gin4, we are removing regulatory regions that may be required to bind and regulate proteins required for driving normal cell growth and growth rate.

From the mass spectrometry experiment in chapter 3, we identified that Gin4 binds to subunits of the TORC2 complex, which is implied to regulate cell growth and growth rate (Schmelzle 2000, Lucena 2018). It is entirely possible that as Gin4 becomes active, it also signals a positive feedback loop to TORC2 to promote further

cell growth in mitosis. The Ypk1 and Ypk2 kinases are directly phosphorylated by TORC2 (Niles 2012), so these phosphorylation events behave as readouts of TORC2 activity and could specifically imply cell growth regulation. Therefore, to test if Gin4 stimulates TORC2 activity to promote cell growth in mitosis, we could look for changes in Ypk1/2 phosphorylation when we overexpress cells harboring C-terminal truncations of Gin4 compared to wild type cells. We would expect to see a decrease in Ypk1/2 phosphorylation if growth rate reduction in Gin4 C-terminal truncations was due to reduced TORC2 activity. However, we also believe that cell growth itself is driving Gin4 phosphorylation during metaphase. It is possible that as Gin4 becomes phosphorylated, partial activity over time is sufficient to stimulate TORC2 activity to drive the cell growth that promotes Gin4 phosphorylation and activation. In previous studies in our lab, Ypk1 phosphorylation starts right when cells are entering mitosis, which provides evidence that TORC2 activity could be stimulating cell growth in metaphase and therefore influencing Gin4 phosphorylation (Alcaide-Galivan 2018). In addition, deleting Gin4 and its redundant paralogs does result in a reduction of Ypk1 phosphorylation right when cells are shifted from a rich to poor nutrient source. However, cells eventually adjust to a partial Ypk1 phosphorylation (Alcaide-Galivan 2018). Reduction of Ypk1 phosphorylation by TORC2 is more obvious in the absence of Elm1 (Alcaide-Galivan 2018), which is required for Gin4 phosphorylation and activation, supporting a model in which Gin4 feedbacks to TORC2 to promote cell growth. The TORC2 complex may be targeting other proteins other than Ypk1, so it is possible that Gin4 promotes TORC2 activity biased another

target protein. However, Ypk1 phosphorylation is required for synthesis of ceramides that are important precursors to complex sphingolipids that are deposited to the plasma membrane for membrane growth (Dickson 2008, Breslow 2010). It is not clear then why we still observe minimal TORC2 activity in the absence of Gin4, besides that TORC2 may be targeting other proteins in a Gin4-dependent manner as it becomes gradually activated in response to cell growth.

Another possible model that could explain how Gin4 promotes its own activation in response to cell growth is by gradually stimulating ribosome biogenesis. The process of ribosome biogenesis promotes cell growth by generating biomass in the form of proteins, but also promotes production of proteins responsible for driving the processes of cell growth (Kafri 2016). The counterpart of TORC2, the TORC1 complex, is a key complex in stimulating ribosome biogenesis (Mayer and Grummt 2006). Both TORC1 and protein kinase A (PKA) work together to target the regulation of key ribosomal proteins, ribosome biogenesis factors, and ribosomal RNAs (Kunkel and Luo 2019). TORC1's activity on ribosome biogenesis also leads to control of cytoplasmic crowding density, which is tightly regulated during cell growth (Delarue 2018). With this context in mind, TORC1 could be stimulated by Gin4 as it gets gradually phosphorylated and activated in response to cell growth. Our mass spectrometry experiment, in chapter 3, identified Tor1, the kinase subunit of the TORC1 complex and other of its subunits as Gin4 binding partners. To really determine if TORC1 is a target of Gin4, we can carry out an *in vitro* assays where we measure the extent of radioactive P^{32} incorporation into TORC1 subunits with and

without the presence of Gin4. The last possibility is that Gin4 stimulates both TORC1 and TORC2 activity to drive ribosome biogenesis and cell growth to promote its own activation via hyperphosphorylation.

Materials and Methods

Yeast strain construction, media, and reagents

All the yeast strains are in the W303 background (leu2-3, 112 ura3-1, can1-100, ade2-1, his3-11, 15 trp1-1, GAL+, ssd1-d2). Yeast cells were grown in YP medium (yeast extract, peptone, 40 mg/L adenine) supplemented with galactose (YPGAL). To generate yeast strains, gene deletion was performed by standard PCR amplification and homologous recombination. Briefly, all Gin4 C-terminal truncation strains were developed by the transformation of a PCR-amplified DNA fragment with 40 bp homologous arms of the GIN4 gene outside its coding region, depending on the truncation, with a TRP nutritional selection marker. All strains contained a GAL1 promoter in front of the GIN4 gene and a 3xHA epitope tag at the C-terminal region of GIN4. Clones were grown in YPGAL media to log-phase overnight at room temperature and probed for HA-tagged GIN4 to test for successful truncations via western blotting. The appearance of an HA-tagged protein band was indicative of a successful GIN4 truncation. All other strains mentioned in this chapter were previously constructed by the Kellogg Lab and in stock.

Cell size analysis of Gin4 C-terminal truncation yeast strains

Wild type and Gin4 C-terminal truncation yeast strains were grown in YEP growth medium supplemented with 2% galactose overnight at room temperature until cells reached log-phase. A milliliter of cells, per strain, were fixed with 100 µLof 37% formaldehyde solution for 15 minutes in a room temperature rotator. Cells were then pelleted and resuspend in 1x PBS + 0.5% Tween-20 + 0.01% Azide solution twice. Cells size was measured using a coulter counter under normal settings for yeast.

Swe1 phosphorylation and mitotic progression *in vivo* assays

Cell cycle time course experiments with these were conducted as previously described (Harvey et al. 2011). Briefly, wild type and C-terminal Gin4 truncation cells were grown in YEP medium (yeast extract, peptone) supplemented with glycerol/ethanol mixture to 2% final concentration at room temperature for 12-16 hours until cells reached an optical density (OD_{600}) between 0.4-0.7. Cells were then pelleted and washed into YPGAL media (yeast extract, peptone, and 2% galactose. Cells were synchronized at G1 phase by treating cells for 3 hours at room temperature with alpha mating factor to a final concentration of 0.5 µg /mL. Cells were released from a G1 arrest by three rounds of pelleting followed by resuspension with an equal volume of YPGAL medium. After the final wash, cells were transferred to 25 ˚C. Starting at 40 minutes, depending on experiment, after release from G1 arrest, 1.6 mL samples were collected every 10 minutes until a total of 120 minutes were reached.

To ensure one cell cycle event was tracked, alpha factor was added at the same volume, again, at 60 minutes after G1 arrest release. Samples were processed for SDS-PAGE gel electrophoresis and western blotting by: Pelleted cells followed by removal of supernatant. Acid-washed microbeads were added to the pellet and flash-freeze in liquid nitrogen. Cells were lysed by adding 140 µg of 1x sample buffer (65 mM Tris-HCl pH 6.8, 3% SDS, 10% glycerol, 5% beta-mercapethanol, and bromophenol blue) supplemented with 2 mM PMSF and placed in a mini-beadbeater 16 (BioSpec) at top speed for 2 minutes at 4 ˚C. After, samples were centrifuged followed by boiling at 95 ˚C for 5 minutes, then, centrifuged again for 5 minutes at 15,000 rpm using a table-top microcentrifuge. Protein samples (10 µL) were separated by passing 20 mA of current through a 10% polyacrylamide gel submerged in running buffer (Glycine, Tris base, 10% SDS), then transferred to a nitrocellulose membrane at 4 C using a wet transfer apparatus at 800 mA in 1x transfer buffer (Tris base, glycine, and methanol) when probing for Swe1 and Clb2. Blots were probed with primary antibody at 1-2 µg/mL overnight at 4 ˚C in 5% milk in PBST (1x phosphate-buffered saline, 250 mM NaCl, and 0.1% Tween-20) containing 5% nonfat dry milk. Primary antibodies were detected by using an HRP-conjugated donkey anti-rabbit secondary antibody incubated in 5% milk PBST solution for 1 hour at room temperature. Blots were rinsed in 1x PBST, followed by a final wash in 1x PBS before detection via chemiluminescence using ECL reagents with a Bio-rad ChemiDoc imaging system.

Growth rate assays

Cell cycle experiments were conducted as described above. Samples were processed every 10 minutes for cell size analysis as described above.

Figures

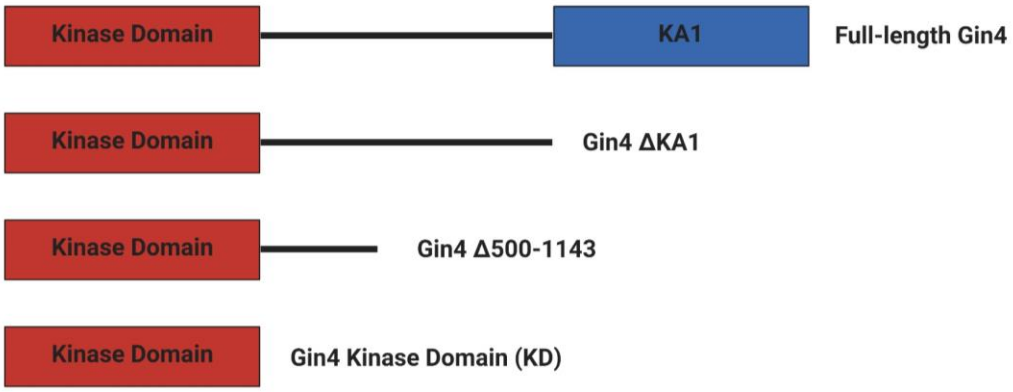

Figure 1. Schematic of Gin4 C-terminal truncations. Shown here are the Gin4 C-terminal truncations we introduced in individual yeast strains to study the effects on cell size and mitotic progression. Full-length Gin4 is shown for reference with the N-terminal kinase domain labeled in red and the C-terminal KA1 anionic phospholipid binding site labeled in blue. The flexible linker is shown as a thick black line between the Kinase and KA1 domains. Sequential truncations are labeled from top to bottom.

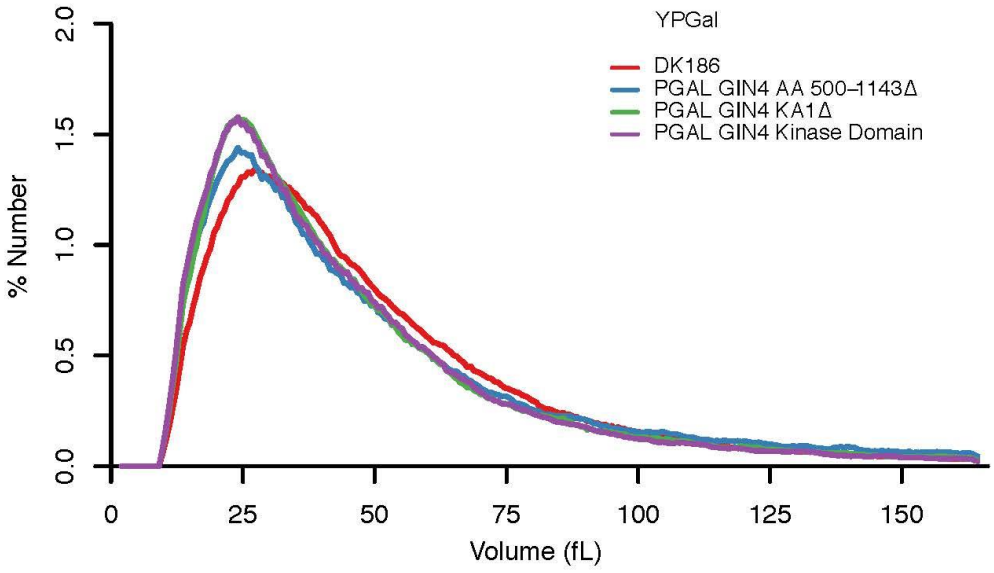

Figure 2. Effects on cell size in Gin4 C-terminal truncation yeast strains. Wild type and Gin4 C-terminal truncation yeast cells were grown in YEP growth medium, supplemented with 2% galactose (YPGAL), overnight to log-phase at room temperature. Cells were then processed for coulter counter cell size measurements the next day. Shown here is a cell size coulter counter plot. The x-axis corresponds to cell size measured as volume (fL) and the y-axis corresponds to the % number of cells within a certain cell volume. The mean cell size of each yeast strain is shown as a peak curve. The cell size curves are labeled as: Wild type (DK186) (red), Gin4 ΔKA1 (green), Gin4 Δ500-1143 (blue), and Gin4 kinase domain (purple). This coulter counter plot corresponds to an experiment with an n = 3.

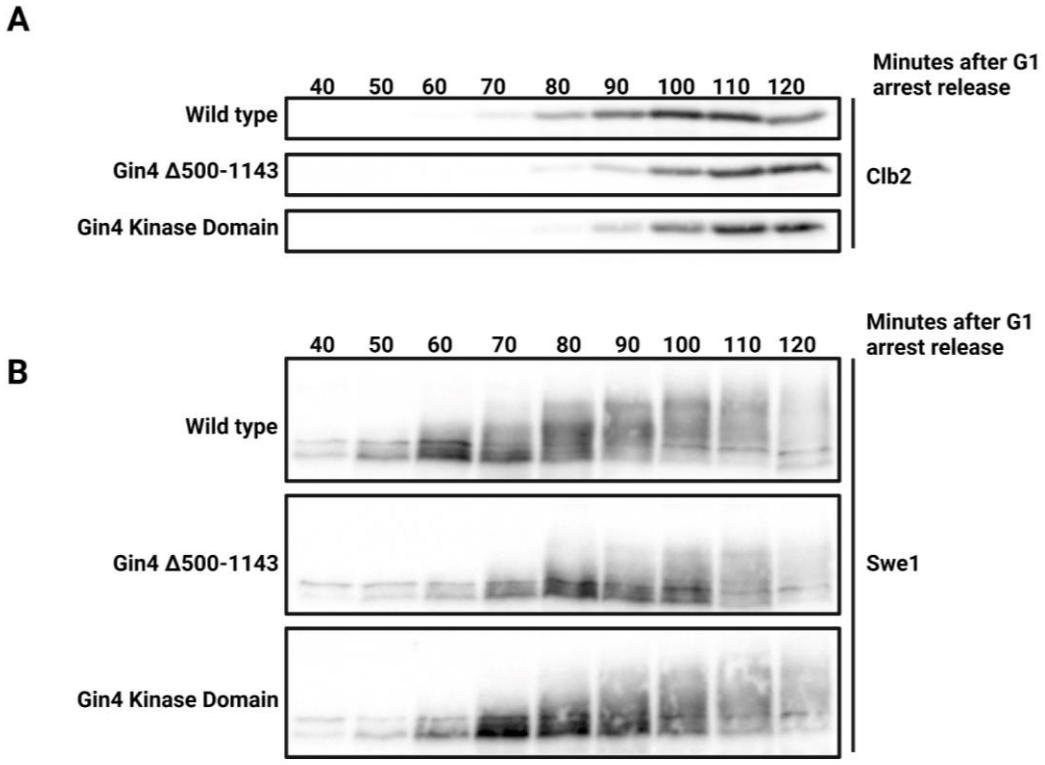

Figure 3. Effects on mitotic progression in Gin4 C-terminal truncation yeast strains. Wild type and Gin4 C-terminal truncation yeast cells were released from a G1 arrest in YEP + 2% galactose (YPGAL) growth medium at room temperature. Samples were collected and processed every 10 minutes. Changes in Clb2 and Swe1, protein levels and phosphorylation, respectively, were tracked via western blotting. The blots shown above are representative of an n=3 experiment.

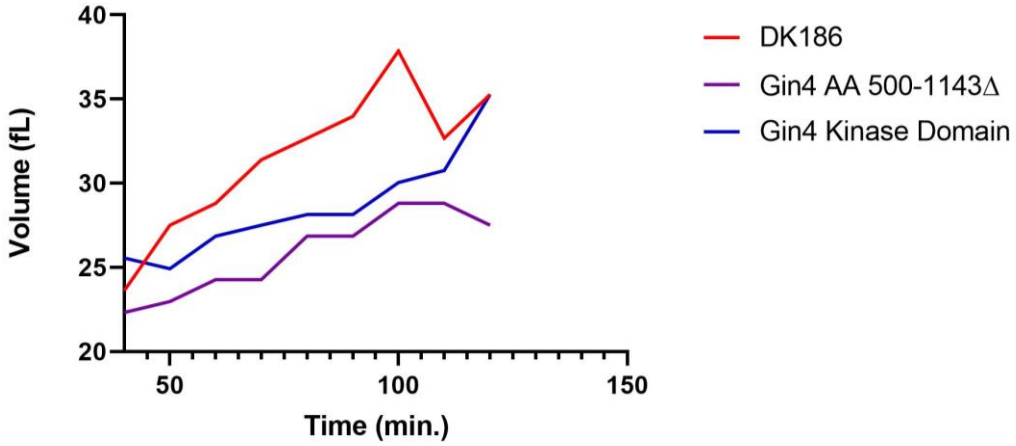

Figure 4. Effects on growth rate in Gin4 C-terminal truncation yeast strains. Wild type and Gin4 C-terminal truncation yeast cells were released from a G1 arrest in YEP + 2% galactose (YPGAL) growth medium at room temperature. Samples were collected and processed every 10 minutes for cell size measurements. Growth rate changes were determined by dividing the mean cell size at that time point over the time cells spent growing. The blots shown above are representative of an n=3 experiment.

Chapter 5: Structural Model of a Gin4-Nap1 complex in the G1 phase of the cell cycle

Introduction

While we have *in vivo* and *in vitro* data explaining how Gin4 phosphorylation and activation may occur, we do not fully understand how these phosphorylation events influence the structure and function of Gin4 throughout the cell cycle. Cryo-EM is an excellent tool to study oligomeric states and conformational changes of purified Gin4 from yeast cells at different stages of the cell cycle. That is because it is a high molecular weight protein that should be visible under a transmission electron microscope (TEM), even individual domains of Gin4 could be analyzed using this technique. In terms of what we know about Gin4 oligomerization *in vivo*, we know that Gin4-Gin4 interactions can occur in mitosis, but not in G1 phase (Mortensen 2002). However, it is unclear what level of oligomerization Gin4 undergoes (e.g., dimer, trimer, etc). In terms of conformational changes that Gin4 may undergo as the cell cycle progresses, it is thought that Gin4 exists in a closed conformation at G1, and once it is fully hyperphosphorylated it is in an open conformation, where it can bind downstream substrate. This hypothesis is based on the MARK/PARK activation model discussed in the introduction of this thesis. We attempted to purify Gin4 complexes from mitotic-arrested yeast cells, however, the MBP-8xHis tag at its C-terminus seemed to disrupt known interactions with the septins. Instead, we opted to attempt to determine a structure of MBP-8xHis tagged Gin4 in complex with Nap1 from log-phase yeast cells since we know that Nap1 binds strongly to Gin4 (Altman

1997, Mortensen 2002), which are predominantly stationed in G1 phase of the cell cycle. Currently, we do not know why Nap1 binds to Gin4 and how it promotes Gin4 kinase activity. However, what we learn about Gin4 structural dynamics using cryo-EM will allow us to understand how growth signals influence Gin4 phosphorylation events at the structural level and maybe a possible role for Nap1 binding to Gin4but also determine if Gin4 exists in conformations based on the MARK/PARK activation model.

Results

Brief Summary of Cryo-EM workflow for structural analysis of Gin4-Nap1 complex

Prior to establishing a protocol for visualizing a Gin4-Nap1 complex under an electron microscope, there were concerns of sample concentration, since cryo-EM is used to determine structures of recombinant proteins expressed in systems other than their native systems to achieve high purity and high concentration. However, expressing and reconstituting a Gin4-Nap1 protein complex from *E. coli* was not a viable option for us, due to Gin4 degradation issues during the purification process. Instead, we took advantage of our established MBP-8xHis-tagged Gin4 yeast strain to purify Gin4-Nap1 complexes from endogenous (not overexpressed Gin4 protein). Purification and concentration of Gin4-Nap1 complexes from log-phase yeast cells were confirmed by coomassie staining (Figure 1). We left the MBP-8xis tag on Gin4 due to instability of the protein after tag removal with TEV protease. We were able to

achieve high purity of Gin4-Nap1 complexes and obtained a reasonable concentration for cryo-EM studies. We first conducted negative stain EM to determine that we can visualize protein particles (not shown). Briefly, small drops of Gin4-Nap1 complexes at 0.2 mg/mL were loaded onto gold grids, frozen in liquid nitrogen, and particles were imaged using an electron microscope, followed by structure analysis.

Overall predicted structure of the Gin4-Nap1 complex

Using software analysis, we obtained a collection of 2D classifications of the Gin4-Nap1 protein complex, which are average structural orientations of the protein complex. From the 2D classification data, we can clearly see flexibility of the complex (Figure 2). Due to high flexibility of the complex, we were not able to obtain an accurate three-dimensional electron map for further analysis and structure determination. However, we can still determine an overall predicted structure of the Gin4-Nap1 complex. From the 2D classification data, a subset of orientations is shown as four "blobs" or folded polypeptides (Figure 2). We predict that these masses of protein correspond to Nap1, the N-terminal Gin4 kinase domain, the C-terminal Gin4 KA1 lipid binding domain, and the MBP-8xHis tag hanging out of the KA1 Gin4 domain.

In the future, confirmation of the MBP-8xHis tag could be obtained by using an MBP-specific antibody in our cryo-EM studies of the Gin4-Nap1 complex. How Nap1 binds Gin4, through direct interactions with the kinase, KA1 domain, flexible linker, or a combination of these domains, is not clear from the 2D classification data.

Determining the structure of the Gin4-Nap1 complex at the atomic level is required to determine binding interfaces between Gin4 and Nap1. Future cryo-EM studies will require modifications to the protocol to obtain Gin4 that is not flexible. The flexibility we observed in our data could be due to three possible reasons: 1) MBP-8xHis tag (43.6 kDa) is highly flexible, 2) The linker domain (629 amino acids forming the domain) of Gin4 found between the kinase and KA1 domains is predicted to be a highly flexible and disordered region, 3) A reagent or condition from the purification protocol or grid freezing conditions is inducing non-specific conformational changes of the protein complex Although, we can't rule out that the flexible linker and its flexibility is required for normal function of Gin4. We thought about possibly removing the flexible linker of Gin4, but this is the region predicted to be highly phosphorylated and could include regions that bind Nap1. Therefore, removing the flexible linker for cryo-EM studies may not be a viable option for us. In terms of oligomerization of Gin4, we did not see any structural patterns in the 2D classification data that suggest that Gin4-Gin4 interactions occur in G1 phase, which is consistent with Co-IP data showing that Gin4 and Nap1 do not bind in G1 (Mortensen 2002).

We predict two possible models for a Gin4-Nap1 complex in G1: 1) A structure in which the kinase domain and KA1 domains interact with each other to induce a closed-state confirmation of Gin4, in complex with Nap1, 2) A Gin4-Nap1 complex structure that is highly flexible in G1 due to its interdomain linker, making Gin4 inactive because its Gin4 kinase domain move so much that a the kinase

domain is unable to efficiently bind downstream substrates.. In both hypothetical models, Gin4 eventually becomes accessible to bind substrate in mitosis in complex with the septins and other proteins required for Gin4 activation. Even though we did not solve the structure of the Gin4-Nap1 complex yet, we were able to infer possible structural models that could explain why Gin4 is in an inactive, dephosphorylated state in G1 phase of the cell cycle.

Materials and Methods

Purification of Gin4-Nap1 complex from yeast

The Gin4-Nap1 complex was purified as described in the chapter 2 methods section. For cryo-EM screening, the Gin4-Nap1 complex was purified with the MBP-8xHis tagged intact.

Negatively stained imaging by transmission electron microscopy (TEM)

For TEM imaging, 3.5 µL of sample aliquots were spotted onto freshly glow-discharged carbon-coated electron microscopy grids (Ted Pella, Catalog No. 01701-F). The grids were rinsed with milliQ water after 30 s incubation, followed by staining with µL 0.75% uranyl formate for 30 s, blotting, and air-drying. Images were recorded at – 2.5 µm defocus at 73,000x magnification using a Thermo Fisher Glacios cryo-TEM operating at 200 kV coupled to a Ceta 16 MP CCD detector. Images were analyzed using ImageJ.

Sample preparation for single-particle cryo-EM and data collection

Purified Gin4-Nap1 complex was concentrated to 0.2 mg/mLat 4 °C and an aliquot of 3.5 µL was deposited on a plasma cleaned (Easy Pelco Glow-discharger)

UltrAUfoil R 1.2/1.3 300 mesh (EM Sciences). Protein excess was blotted for 1.5 s with a force of −10 and 100% humidity before being plunged frozen into liquid ethane using the Vitrobot Mark IV (Thermo Fisher) located at the Biomolecular cryoEM facility at UC – Santa Cruz. Frozen grids were screened in Glacios (Thermo Fisher) at 200 kV equipped with a Gatan K2 Summit direct detector.

The dataset was collected at a resolution mode, with a nominal pixel size of 0.6915 Å/pix (57,000x magnification), a stack of 59 frames, and a total dose of 69.2 $e^{-}/Å^{2}$. A total of 1326 movies were collected and further processed using cryoSPARC v3.2.

Single-particle cryo-EM data processing

Pre-processing patch motion correction and CTF correction were performed at cryoSPARC v.3.2. Circular blob picking was performed using the 20-50 Å range and cropped at 240 pixels. The particles were further selected through 2D classification, resulting in 418,756 particles used at the initial 3D classification. Particles belonging to the representative group were submitted to another 2D classification round for further cleaning and submitted to non-uniform refinement. Again, due to high flexibility of the protein, a 3-D reconstruction map of the Gin4 kinase was not achieved.

Figures

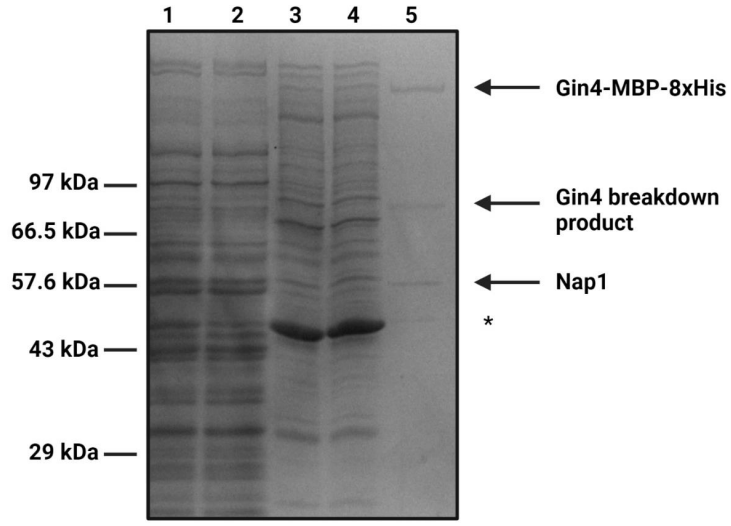

Figure 1. Coomassie-stained gel image of purified Gin4-Nap1 complex. Gin4-Nap1 complex was purified from log-phase yeast cells using a two-step chromatography process. In lane 1 is the cell extract, lane 2 is the flow-through from a nickel column, lane 3 is eluate from nickel column, lane 4 is flow through from an amylose column, and lane 5 is our final purified Gin4-Nap1 complex from an amylose column. There is a major Gin4 breakdown product below 97 kDa. The asterisk (*) denotes a contaminating protein that was not identified.

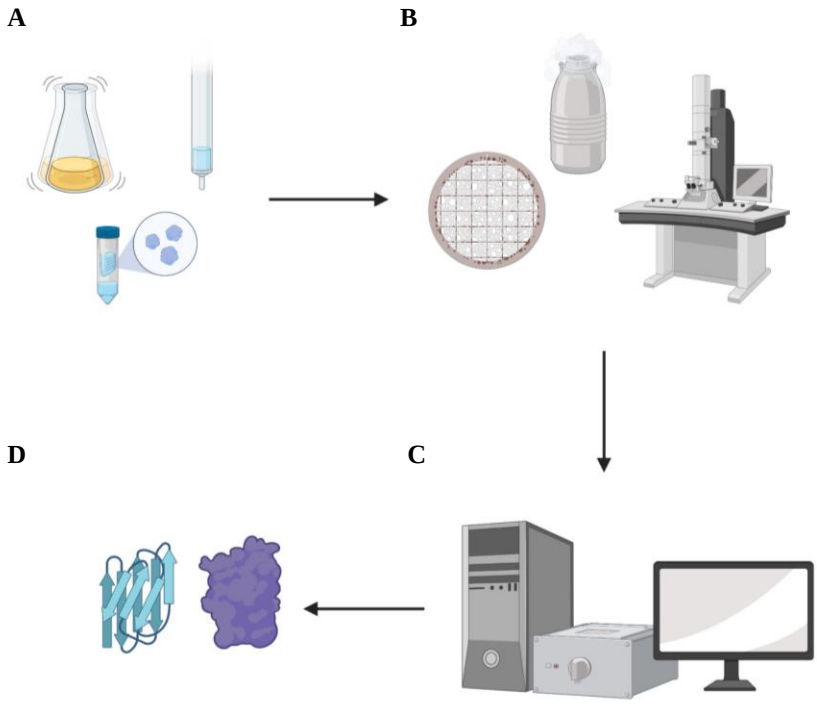

Figure 2. Schematic of Cryo-EM workflow. A) Purification of MBP-8xHis tagged Gin4-Nap1 complex, B) Grid preparation and particle screening under TEM, C) Data Processing, D) 3-D structure determination

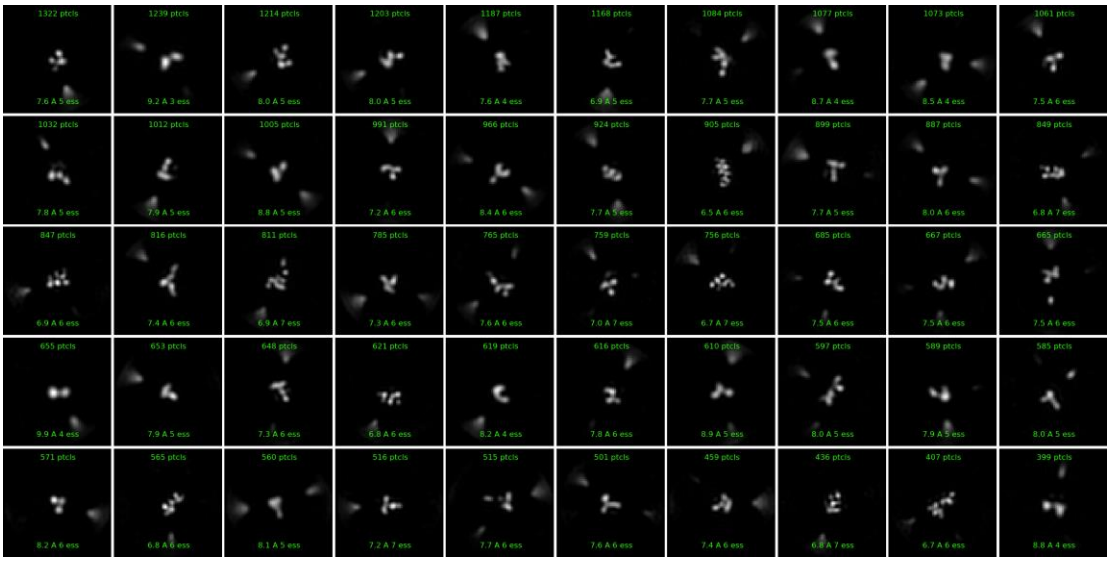

Figure 3. 2D Classifications of Gin4-Nap1 particles. From data analysis and processing, these 2-D classification were obtained. Each box represents an average orientation of the Gin4-Nap1 particle. Shown above are examples of highly flexible particles and stable particles, but it is possible that the particles in blue boxes may be due to how they sit on the grid.

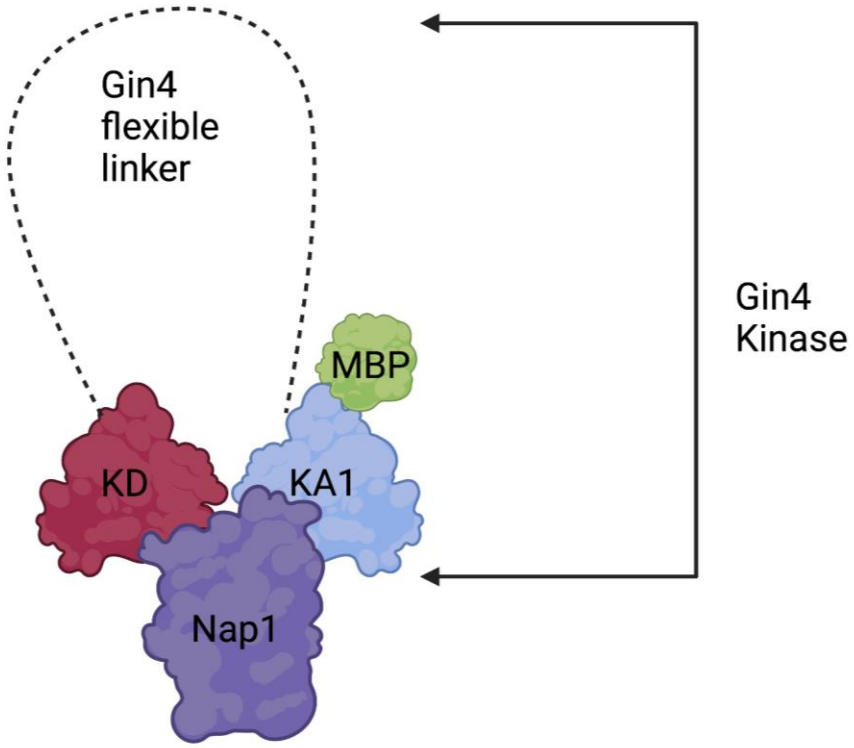

Figure 4. Model of Gin4-Nap1 structure in G1 phase of the cell cycle. Based on the 2-D classification data, the Gin4-Nap1 particles appear to consist of four "blobs". Our prediction is the kinase domain (red blob) interacts with the KA1 domain (light blue blob) resulting in a closed conformation of the Gin4 kinase. The flexible interdomain linker of Gin4 is highlighted in dashed line. Nap1 (purple blob) is predicted to be in complex with a single molecule of Gin4 kinase, but how it interacts cannot be predicted here. The MBP-8xHis tag is highlighted as a green blob here.

Bibliography

Chapter 1

Altman, R., & Kellogg, D. (1997). Control of mitotic events by Nap1 and the Gin4 kinase. *The Journal of Cell Biology*, *138*(1), 119–130. https://doi.org/10.1083/jcb.138.1.119

Anastasia, S. D., Nguyen, D. L., Thai, V., Meloy, M., MacDonough, T., & Kellogg, D. R. (2012). A link between mitotic entry and membrane growth suggests a novel model for cell size control. *The Journal of Cell Biology*, *197*(1), 89–104. https://doi.org/10.1083/jcb.201108108

Babu, P., Bryan, J. D., Panek, H. R., Jordan, S. L., Forbrich, B. M., Kelley, S. C., Colvin, R. T., & Robinson, L. C. (2002). Plasma membrane localization of the Yck2p yeast casein kinase 1 isoform requires the C-terminal extension and secretory pathway function. *Journal of Cell Science*, *115*(24), 4957–4968. https://doi.org/10.1242/jcs.00203

Campos, M., Surovtsev, I. V., Kato, S., Paintdakhi, A., Beltran, B., Ebmeier, S. E., & Jacobs-Wagner, C. (2014). A constant size extension drives bacterial cell size homeostasis. *Cell*, *159*(6), 1433–1446. https://doi.org/10.1016/j.cell.2014.11.022

Coleman, T. R., Tang, Z., & Dunphy, W. G. (1993). Negative regulation of the wee1 protein kinase by direct action of the nim1/cdr1 mitotic inducer. *Cell*, *72*(6), 919–929. https://doi.org/10.1016/0092-8674(93)90580-j

Emptage, R. P., Lemmon, M. A., & Ferguson, K. M. (2017). Molecular determinants of KA1 domain-mediated autoinhibition and phospholipid activation of MARK1 kinase. *The Biochemical Journal*, *474*(3), 385–398. https://doi.org/10.1042/BCJ20160792

Emptage, R. P., Lemmon, M. A., Ferguson, K. M., & Marmorstein, R. (2018). Structural Basis for MARK1 Kinase Autoinhibition by Its KA1 Domain. *Structure (London, England: 1993)*, *26*(8), 1137-1143.e3. https://doi.org/10.1016/j.str.2018.05.008

Facchetti, G., Chang, F., & Howard, M. (2017). Controlling cell size through sizer mechanisms. *Current Opinion in Systems Biology*, *5*, 86–92. https://doi.org/10.1016/j.coisb.2017.08.010

Ginzberg, M. B., Kafri, R., & Kirschner, M. (2015a). Cell biology. On being the right (cell) size. *Science (New York, N.Y.)*, *348*(6236), 1245075. https://doi.org/10.1126/science.1245075

Ginzberg, M. B., Kafri, R., & Kirschner, M. (2015b). On being the right (cell) size. *Science*, *348*(6236), 1245075–1245075. https://doi.org/10.1126/science.1245075

Hanrahan, J., & Snyder, M. (2003). Cytoskeletal Activation of a Checkpoint Kinase. *Molecular Cell*, *12*(3), 663–673. https://doi.org/10.1016/j.molcel.2003.08.006

Harvey, S. L., & Kellogg, D. R. (2003). Conservation of mechanisms controlling entry into mitosis: Budding yeast wee1 delays entry into mitosis and is required for cell size control. *Current Biology: CB*, *13*(4), 264–275. https://doi.org/10.1016/s0960-9822(03)00049-6

Jasani, A., Huynh, T., & Kellogg, D. R. (2020). Growth-Dependent Activation of Protein Kinases Suggests a Mechanism for Measuring Cell Growth. *Genetics*, *215*(3), 729–746. https://doi.org/10.1534/genetics.120.303200

Kanoh, J., & Russell, P. (1998). The protein kinase Cdr2, related to Nim1/Cdr1 mitotic inducer, regulates the onset of mitosis in fission yeast. *Molecular Biology of the Cell*, *9*(12), 3321–3334. https://doi.org/10.1091/mbc.9.12.3321

Li, M., Strand, D., Krehan, A., Pyerin, W., Heid, H., Neumann, B., & Mechler, B. M. (1999). Casein kinase 2 binds and phosphorylates the nucleosome assembly protein-1 (NAP1) in Drosophila melanogaster 1 1Edited by M. Yaniv. *Journal of Molecular Biology*, *293*(5), 1067–1084. https://doi.org/10.1006/jmbi.1999.3207

Marx, A., Nugoor, C., Panneerselvam, S., & Mandelkow, E. (2010). Structure and function of polarity-inducing kinase family MARK/Par-1 within the branch of AMPK/Snf1-related kinases. *FASEB Journal: Official Publication of the Federation of American Societies for Experimental Biology*, *24*(6), 1637–1648. https://doi.org/10.1096/fj.09-148064

Moravcevic, K., Mendrola, J. M., Schmitz, K. R., Wang, Y.-H., Slochower, D., Janmey, P. A., & Lemmon, M. A. (2010). Kinase associated-1 domains drive MARK/PAR1 kinases to membrane targets by binding acidic phospholipids. *Cell*, *143*(6), 966–977. https://doi.org/10.1016/j.cell.2010.11.028

Mortensen, E. M., McDonald, H., Yates, J., & Kellogg, D. R. (2002). Cell cycle-dependent assembly of a Gin4-septin complex. *Molecular Biology of the Cell*, *13*(6), 2091–2105. https://doi.org/10.1091/mbc.01-10-0500

Nesić, D., Miller, M. C., Quinkert, Z. T., Stein, M., Chait, B. T., & Stebbins, C. E. (2010). Helicobacter pylori CagA inhibits PAR1-MARK family kinases by mimicking host substrates. *Nature Structural & Molecular Biology*, *17*(1), 130–132. https://doi.org/10.1038/nsmb.1705

Opalko, H. E., Nasa, I., Kettenbach, A. N., & Moseley, J. B. (2019). A mechanism for how Cdr1/Nim1 kinase promotes mitotic entry by inhibiting Wee1. *Molecular Biology of the Cell*, *30*(25), 3015–3023. https://doi.org/10.1091/mbc.E19-08-0430

Schmoller, K. M., Turner, J. J., Kõivomägi, M., & Skotheim, J. M. (2015). Dilution of the cell cycle inhibitor Whi5 controls budding-yeast cell size. *Nature*, *526*(7572), 268–272. https://doi.org/10.1038/nature14908

Soifer, I., Robert, L., & Amir, A. (2016). Single-Cell Analysis of Growth in Budding Yeast and Bacteria Reveals a Common Size Regulation Strategy. *Current Biology*, *26*(3), 356–361. https://doi.org/10.1016/j.cub.2015.11.067

Chapter 2

Altman, R., & Kellogg, D. (1997). Control of mitotic events by Nap1 and the Gin4 kinase. *The Journal of Cell Biology*, *138*(1), 119–130. https://doi.org/10.1083/jcb.138.1.119

Anastasia, S. D., Nguyen, D. L., Thai, V., Meloy, M., MacDonough, T., & Kellogg, D. R. (2012). A link between mitotic entry and membrane growth suggests a novel model for cell size control. *The Journal of Cell Biology*, *197*(1), 89–104. https://doi.org/10.1083/jcb.201108108

Asano, S., Park, J.-E., Yu, L.-R., Zhou, M., Sakchaisri, K., Park, C. J., Kang, Y. H., Thorner, J., Veenstra, T. D., & Lee, K. S. (2006). Direct phosphorylation and activation of a Nim1-related kinase Gin4 by Elm1 in budding yeast. *The Journal of Biological Chemistry*, *281*(37), 27090–27098. https://doi.org/10.1074/jbc.M601483200

Babu, P., Bryan, J. D., Panek, H. R., Jordan, S. L., Forbrich, B. M., Kelley, S. C., Colvin, R. T., & Robinson, L. C. (2002). Plasma membrane localization of the Yck2p yeast casein kinase 1 isoform requires the C-terminal extension and secretory pathway function. *Journal of Cell Science*, *115*(24), 4957–4968. https://doi.org/10.1242/jcs.00203

Babu, P., Deschenes, R. J., & Robinson, L. C. (2004). Akr1p-dependent palmitoylation of Yck2p yeast casein kinase 1 is necessary and sufficient for plasma membrane targeting. *The Journal of Biological Chemistry*, *279*(26), 27138–27147. https://doi.org/10.1074/jbc.M403071200

Budini, M., Jacob, G., Jedlicki, A., Pérez, C., Allende, C. C., & Allende, J. E. (2009). Autophosphorylation of carboxy-terminal residues inhibits the activity of protein

kinase CK1α. *Journal of Cellular Biochemistry*, *106*(3), 399–408. https://doi.org/10.1002/jcb.22019

Cegielska, A., Gietzen, K. F., Rivers, A., & Virshup, D. M. (1998). Autoinhibition of Casein Kinase I ε (CKIε) Is Relieved by Protein Phosphatases and Limited Proteolysis. *Journal of Biological Chemistry*, *273*(3), 1357–1364. https://doi.org/10.1074/jbc.273.3.1357

Emptage, R. P., Lemmon, M. A., & Ferguson, K. M. (2017). Molecular determinants of KA1 domain-mediated autoinhibition and phospholipid activation of MARK1 kinase. *The Biochemical Journal*, *474*(3), 385–398. https://doi.org/10.1042/BCJ20160792

Emptage, R. P., Lemmon, M. A., Ferguson, K. M., & Marmorstein, R. (2018). Structural Basis for MARK1 Kinase Autoinhibition by Its KA1 Domain. *Structure (London, England: 1993)*, *26*(8), 1137-1143.e3. https://doi.org/10.1016/j.str.2018.05.008

Feng, Y., & Davis, N. G. (2000). Akr1p and the type I casein kinases act prior to the ubiquitination step of yeast endocytosis: Akr1p is required for kinase localization to the plasma membrane. *Molecular and Cellular Biology*, *20*(14), 5350–5359. https://doi.org/10.1128/MCB.20.14.5350-5359.2000

Graves, P. R., & Roach, P. J. (1995). Role of COOH-terminal Phosphorylation in the Regulation of Casein Kinase Iδ. *Journal of Biological Chemistry*, *270*(37), 21689–21694. https://doi.org/10.1074/jbc.270.37.21689

Harvey, S. L., Enciso, G., Dephoure, N., Gygi, S. P., Gunawardena, J., & Kellogg, D. R. (2011). A phosphatase threshold sets the level of Cdk1 activity in early mitosis in budding yeast. *Molecular Biology of the Cell*, *22*(19), 3595–3608. https://doi.org/10.1091/mbc.E11-04-0340

Janke, C., Magiera, M. M., Rathfelder, N., Taxis, C., Reber, S., Maekawa, H., Moreno-Borchart, A., Doenges, G., Schwob, E., Schiebel, E., & Knop, M. (2004). A versatile toolbox for PCR-based tagging of yeast genes: New fluorescent proteins, more markers and promoter substitution cassettes. *Yeast*, *21*(11), 947–962. https://doi.org/10.1002/yea.1142

Jasani, A., Huynh, T., & Kellogg, D. R. (2020). Growth-Dependent Activation of Protein Kinases Suggests a Mechanism for Measuring Cell Growth. *Genetics*, *215*(3), 729–746. https://doi.org/10.1534/genetics.120.303200

Longtine, M. S., McKenzie, A., Demarini, D. J., Shah, N. G., Wach, A., Brachat, A., Philippsen, P., & Pringle, J. R. (1998). Additional modules for versatile and economical PCR-based gene deletion and modification in Saccharomyces cerevisiae. *Yeast (Chichester, England)*, *14*(10), 953–961. https://doi.org/10.1002/(SICI)1097-0061(199807)14:10<953::AID-YEA293>3.0.CO;2-U

Moravcevic, K., Mendrola, J. M., Schmitz, K. R., Wang, Y.-H., Slochower, D., Janmey, P. A., & Lemmon, M. A. (2010). Kinase associated-1 domains drive MARK/PAR1

kinases to membrane targets by binding acidic phospholipids. *Cell*, *143*(6), 966–977. https://doi.org/10.1016/j.cell.2010.11.028

Mortensen, E. M., McDonald, H., Yates, J., & Kellogg, D. R. (2002). Cell cycle-dependent assembly of a Gin4-septin complex. *Molecular Biology of the Cell*, *13*(6), 2091–2105. https://doi.org/10.1091/mbc.01-10-0500

Nesić, D., Miller, M. C., Quinkert, Z. T., Stein, M., Chait, B. T., & Stebbins, C. E. (2010). Helicobacter pylori CagA inhibits PAR1-MARK family kinases by mimicking host substrates. *Nature Structural & Molecular Biology*, *17*(1), 130–132. https://doi.org/10.1038/nsmb.1705

Niles, B. J., Mogri, H., Hill, A., Vlahakis, A., & Powers, T. (2012). Plasma membrane recruitment and activation of the AGC kinase Ypk1 is mediated by target of rapamycin complex 2 (TORC2) and its effector proteins Slm1 and Slm2. *Proceedings of the National Academy of Sciences of the United States of America*, *109*(5), 1536–1541. https://doi.org/10.1073/pnas.1117563109

Pasula, S., Chakraborty, S., Choi, J. H., & Kim, J.-H. (2010). Role of casein kinase 1 in the glucose sensor-mediated signaling pathway in yeast. *BMC Cell Biology*, *11*, 17. https://doi.org/10.1186/1471-2121-11-17

Robinson, L. C., Menold, M. M., Garrett, S., & Culbertson, M. R. (1993). Casein Kinase I-Like Protein Kinases Encoded by *YCK1* and *YCK2* are Required for Yeast Morphogenesis. *Molecular and Cellular Biology*, *13*(5), 2870–2881. https://doi.org/10.1128/mcb.13.5.2870-2881.1993

Roth, A. F., Feng, Y., Chen, L., & Davis, N. G. (2002). The yeast DHHC cysteine-rich domain protein Akr1p is a palmitoyl transferase. *The Journal of Cell Biology*, *159*(1), 23–28. https://doi.org/10.1083/jcb.200206120

Sreenivasan, A., & Kellogg, D. (1999). The Elm1 Kinase Functions in a Mitotic Signaling Network in Budding Yeast. *Molecular and Cellular Biology*, *19*(12), 7983–7994. https://doi.org/10.1128/MCB.19.12.7983

Tjandra, H., Compton, J., & Kellogg, D. (1998). Control of mitotic events by the Cdc42 GTPase, the Clb2 cyclin and a member of the PAK kinase family. *Current Biology*, *8*(18), 991–1000. https://doi.org/10.1016/S0960-9822(07)00419-8

Chapter 3

Bandyopadhyay, S., Mehta, M., Kuo, D., Sung, M.-K., Chuang, R., Jaehnig, E. J., Bodenmiller, B., Licon, K., Copeland, W., Shales, M., Fiedler, D., Dutkowski, J., Guénolé, A., van Attikum, H., Shokat, K. M., Kolodner, R. D., Huh, W.-K., Aebersold, R., Keogh, M.-C., … Ideker, T. (2010). Rewiring of genetic networks in response to DNA damage. *Science (New York, N.Y.)*, *330*(6009), 1385–1389. https://doi.org/10.1126/science.1195618

Costanzo, M., Baryshnikova, A., Bellay, J., Kim, Y., Spear, E. D., Sevier, C. S., Ding, H., Koh, J. L. Y., Toufighi, K., Mostafavi, S., Prinz, J., St Onge, R. P., VanderSluis, B., Makhnevych, T., Vizeacoumar, F. J., Alizadeh, S., Bahr, S., Brost, R. L., Chen, Y., … Boone, C. (2010). The genetic landscape of a cell. *Science (New York, N.Y.)*, *327*(5964), 425–431. https://doi.org/10.1126/science.1180823

Costanzo, M., VanderSluis, B., Koch, E. N., Baryshnikova, A., Pons, C., Tan, G., Wang, W., Usaj, M., Hanchard, J., Lee, S. D., Pelechano, V., Styles, E. B., Billmann, M., van Leeuwen, J., van Dyk, N., Lin, Z.-Y., Kuzmin, E., Nelson, J., Piotrowski, J. S., … Boone, C. (2016). A global genetic interaction network maps a wiring diagram of cellular function. *Science (New York, N.Y.)*, *353*(6306), aaf1420. https://doi.org/10.1126/science.aaf1420

Fiedler, D., Braberg, H., Mehta, M., Chechik, G., Cagney, G., Mukherjee, P., Silva, A. C., Shales, M., Collins, S. R., van Wageningen, S., Kemmeren, P., Holstege, F. C. P., Weissman, J. S., Keogh, M.-C., Koller, D., Shokat, K. M., & Krogan, N. J. (2009). Functional organization of the S. cerevisiae phosphorylation network. *Cell*, *136*(5), 952–963. https://doi.org/10.1016/j.cell.2008.12.039

Horsey, E. W., Jakovljevic, J., Miles, T. D., Harnpicharnchai, P., & Woolford, J. L. (2004). Role of the yeast Rrp1 protein in the dynamics of pre-ribosome maturation. *RNA (New York, N.Y.)*, *10*(5), 813–827. https://doi.org/10.1261/rna.5255804

Jasani, A., Huynh, T., & Kellogg, D. R. (2020). Growth-Dependent Activation of Protein Kinases Suggests a Mechanism for Measuring Cell Growth. *Genetics*, *215*(3), 729–746. https://doi.org/10.1534/genetics.120.303200

Jorgensen, P., Rupes, I., Sharom, J. R., Schneper, L., Broach, J. R., & Tyers, M. (2004). A dynamic transcriptional network communicates growth potential to ribosome synthesis and critical cell size. *Genes & Development*, *18*(20), 2491–2505. https://doi.org/10.1101/gad.1228804

Kumar, J., & Kumar, V. (2021). Ribosome proteins—Their balanced production. In *Emerging Concepts in Ribosome Structure, Biogenesis, and Function* (pp. 47–87). Elsevier. https://doi.org/10.1016/B978-0-12-816364-1.00003-2\

Li, Y., Moir, R. D., Sethy-Coraci, I. K., Warner, J. R., & Willis, I. M. (2000). Repression of Ribosome and tRNA Synthesis in Secretion-Defective Cells Is Signaled by a Novel Branch of the Cell Integrity Pathway. *Molecular and Cellular Biology*, *20*(11), 3843–3851. https://doi.org/10.1128/MCB.20.11.3843-3851.2000

Luke, M. M., Della Seta, F., Di Como, C. J., Sugimoto, H., Kobayashi, R., & Arndt, K. T. (1996). The SAP, a new family of proteins, associate and function positively with the SIT4 phosphatase. *Molecular and Cellular Biology*, *16*(6), 2744–2755. https://doi.org/10.1128/MCB.16.6.2744

Mayer, C., & Grummt, I. (2006). Ribosome biogenesis and cell growth: MTOR coordinates transcription by all three classes of nuclear RNA polymerases. *Oncogene*, *25*(48), 6384–6391. https://doi.org/10.1038/sj.onc.1209883

Miles, T. D., Jakovljevic, J., Horsey, E. W., Harnpicharnchai, P., Tang, L., & Woolford, J. L. (2005). Ytm1, Nop7, and Erb1 form a complex necessary for maturation of yeast 66S preribosomes. *Molecular and Cellular Biology*, *25*(23), 10419–10432. https://doi.org/10.1128/MCB.25.23.10419-10432.2005

Mortensen, E. M., McDonald, H., Yates, J., & Kellogg, D. R. (2002). Cell cycle-dependent assembly of a Gin4-septin complex. *Molecular Biology of the Cell*, *13*(6), 2091–2105. https://doi.org/10.1091/mbc.01-10-0500

Nanduri, J., & Tartakoff, A. M. (2001). The Arrest of Secretion Response in Yeast. *Molecular Cell*, *8*(2), 281–289. https://doi.org/10.1016/S1097-2765(01)00312-4

Ptacek, J., Devgan, G., Michaud, G., Zhu, H., Zhu, X., Fasolo, J., Guo, H., Jona, G., Breitkreutz, A., Sopko, R., McCartney, R. R., Schmidt, M. C., Rachidi, N., Lee, S.-J., Mah, A. S., Meng, L., Stark, M. J. R., Stern, D. F., De Virgilio, C., … Snyder, M. (2005). Global analysis of protein phosphorylation in yeast. *Nature*, *438*(7068), 679–684. https://doi.org/10.1038/nature04187

Schmelzle, T., & Hall, M. N. (2000). TOR, a central controller of cell growth. *Cell*, *103*(2), 253–262. https://doi.org/10.1016/s0092-8674(00)00117-3

Sharifpoor, S., van Dyk, D., Costanzo, M., Baryshnikova, A., Friesen, H., Douglas, A. C., Youn, J.-Y., VanderSluis, B., Myers, C. L., Papp, B., Boone, C., & Andrews, B. J. (2012). Functional wiring of the yeast kinome revealed by global analysis of genetic network motifs. *Genome Research*, *22*(4), 791–801. https://doi.org/10.1101/gr.129213.111

Shimoji, K., Jakovljevic, J., Tsuchihashi, K., Umeki, Y., Wan, K., Kawasaki, S., Talkish, J., Woolford, J. L., & Mizuta, K. (2012). Ebp2 and Brx1 function cooperatively in

60S ribosomal subunit assembly in Saccharomyces cerevisiae. *Nucleic Acids Research*, *40*(10), 4574–4588. https://doi.org/10.1093/nar/gks057

Visintin, R., Craig, K., Hwang, E. S., Prinz, S., Tyers, M., & Amon, A. (1998). The phosphatase Cdc14 triggers mitotic exit by reversal of Cdk-dependent phosphorylation. *Molecular Cell*, *2*(6), 709–718. https://doi.org/10.1016/s1097-2765(00)80286-5

Chapter 4

Alcaide-Gavilán, M., Lucena, R., Schubert, K. A., Artiles, K. L., Zapata, J., & Kellogg, D. R. (2018). Modulation of TORC2 Signaling by a Conserved Lkb1 Signaling Axis in Budding Yeast. *Genetics*, *210*(1), 155–170. https://doi.org/10.1534/genetics.118.301296

Breslow, D. K., & Weissman, J. S. (2010). Membranes in balance: Mechanisms of sphingolipid homeostasis. *Molecular Cell*, *40*(2), 267–279. https://doi.org/10.1016/j.molcel.2010.10.005

Coleman, T. R., Tang, Z., & Dunphy, W. G. (1993). Negative regulation of the wee1 protein kinase by direct action of the nim1/cdr1 mitotic inducer. *Cell*, *72*(6), 919–929. https://doi.org/10.1016/0092-8674(93)90580-j

Delarue, M., Brittingham, G. P., Pfeffer, S., Surovtsev, I. V., Pinglay, S., Kennedy, K. J., Schaffer, M., Gutierrez, J. I., Sang, D., Poterewicz, G., Chung, J. K., Plitzko, J. M., Groves, J. T., Jacobs-Wagner, C., Engel, B. D., & Holt, L. J. (2018). MTORC1 Controls Phase Separation and the Biophysical Properties of the Cytoplasm by Tuning Crowding. *Cell*, *174*(2), 338-349.e20. https://doi.org/10.1016/j.cell.2018.05.042

Dickson, R. C. (2008). Thematic review series: Sphingolipids. New insights into sphingolipid metabolism and function in budding yeast. *Journal of Lipid Research*, *49*(5), 909–921. https://doi.org/10.1194/jlr.R800003-JLR200

Dunphy, W. G., & Kumagai, A. (1991). The cdc25 protein contains an intrinsic phosphatase activity. *Cell*, *67*(1), 189–196. https://doi.org/10.1016/0092-8674(91)90582-j

Emptage, R. P., Lemmon, M. A., & Ferguson, K. M. (2017). Molecular determinants of KA1 domain-mediated autoinhibition and phospholipid activation of MARK1 kinase. *The Biochemical Journal*, *474*(3), 385–398. https://doi.org/10.1042/BCJ20160792

Gautier, J., Solomon, M. J., Booher, R. N., Bazan, J. F., & Kirschner, M. W. (1991). Cdc25 is a specific tyrosine phosphatase that directly activates p34cdc2. *Cell*, *67*(1), 197–211. https://doi.org/10.1016/0092-8674(91)90583-k

Gould, K. L., & Nurse, P. (1989). Tyrosine phosphorylation of the fission yeast cdc2+ protein kinase regulates entry into mitosis. *Nature*, *342*(6245), 39–45. https://doi.org/10.1038/342039a0

Harvey, S. L., Charlet, A., Haas, W., Gygi, S. P., & Kellogg, D. R. (2005). Cdk1-dependent regulation of the mitotic inhibitor Wee1. *Cell*, *122*(3), 407–420. https://doi.org/10.1016/j.cell.2005.05.029

Harvey, S. L., Enciso, G., Dephoure, N., Gygi, S. P., Gunawardena, J., & Kellogg, D. R. (2011). A phosphatase threshold sets the level of Cdk1 activity in early mitosis in budding yeast. *Molecular Biology of the Cell*, *22*(19), 3595–3608. https://doi.org/10.1091/mbc.E11-04-0340

Jasani, A., Huynh, T., & Kellogg, D. R. (2020). Growth-Dependent Activation of Protein Kinases Suggests a Mechanism for Measuring Cell Growth. *Genetics*, *215*(3), 729–746. https://doi.org/10.1534/genetics.120.303200

Kunkel, J., Luo, X., & Capaldi, A. P. (2019). Integrated TORC1 and PKA signaling control the temporal activation of glucose-induced gene expression in yeast. *Nature Communications*, *10*(1), 3558. https://doi.org/10.1038/s41467-019-11540-y

Lucena, R., Alcaide-Gavilán, M., Schubert, K., He, M., Domnauer, M. G., Marquer, C., Klose, C., Surma, M. A., & Kellogg, D. R. (2018). Cell Size and Growth Rate Are Modulated by TORC2-Dependent Signals. *Current Biology: CB*, *28*(2), 196-210.e4. https://doi.org/10.1016/j.cub.2017.11.069

Mayer, C., & Grummt, I. (2006). Ribosome biogenesis and cell growth: MTOR coordinates transcription by all three classes of nuclear RNA polymerases. *Oncogene*, *25*(48), 6384–6391. https://doi.org/10.1038/sj.onc.1209883

Mueller, P. R., Coleman, T. R., & Dunphy, W. G. (1995). Cell cycle regulation of a Xenopus Wee1-like kinase. *Molecular Biology of the Cell*, *6*(1), 119–134. https://doi.org/10.1091/mbc.6.1.119

Niles, B. J., Mogri, H., Hill, A., Vlahakis, A., & Powers, T. (2012). Plasma membrane recruitment and activation of the AGC kinase Ypk1 is mediated by target of rapamycin complex 2 (TORC2) and its effector proteins Slm1 and Slm2. *Proceedings of the National Academy of Sciences of the United States of America*, *109*(5), 1536–1541. https://doi.org/10.1073/pnas.1117563109

Schmelzle, T., & Hall, M. N. (2000). TOR, a central controller of cell growth. *Cell*, *103*(2), 253–262. https://doi.org/10.1016/s0092-8674(00)00117-3

Chapter 5

Mortensen, E. M., McDonald, H., Yates, J., & Kellogg, D. R. (2002). Cell cycle-dependent assembly of a Gin4-septin complex. *Molecular Biology of the Cell*, *13*(6), 2091–2105. https://doi.org/10.1091/mbc.01-10-0500